A New Facet of Vitamin B_{12}: Gene Regulation by Cobalamin-Based Photoreceptors

S. Padmanabhan,[1] Marco Jost,[2,3] Catherine L. Drennan,[2,4] and Montserrat Elías-Arnanz[5]

[1]Instituto de Química Física Rocasolano, Consejo Superior de Investigaciones Científicas, 28006 Madrid, Spain; email: padhu@iqfr.csic.es

[2]Department of Chemistry, Massachusetts Institute of Technology, Cambridge, Massachusetts 02139

[3]Department of Cellular and Molecular Pharmacology, University of California, San Francisco, California 94158-2140; email: marco.jost@ucsf.edu

[4]Department of Biology and Howard Hughes Medical Institute, Massachusetts Institute of Technology, Cambridge, Massachusetts 02139; email: cdrennan@mit.edu

[5]Departamento de Genética y Microbiología, Área de Genética, Unidad Asociada al Instituto de Química Física Rocasolano, Consejo Superior de Investigaciones Científicas, Facultad de Biología, Universidad de Murcia, 30100 Murcia, Spain; email: melias@um.es

Annu. Rev. Biochem. 2017. 86:485–514

The *Annual Review of Biochemistry* is online at biochem.annualreviews.org

https://doi.org/10.1146/annurev-biochem-061516-044500

Keywords

photoregulation, photochemistry, CarH, transcriptional repressor, chromophore, optogenetics

Abstract

Living organisms sense and respond to light, a crucial environmental factor, using photoreceptors, which rely on bound chromophores such as retinal, flavins, or linear tetrapyrroles for light sensing. The discovery of photoreceptors that sense light using 5′-deoxyadenosylcobalamin, a form of vitamin B_{12} that is best known as an enzyme cofactor, has expanded the number of known photoreceptor families and unveiled a new biological role of this vitamin. The prototype of these B_{12}-dependent photoreceptors, the transcriptional repressor CarH, is widespread in bacteria and mediates light-dependent gene regulation in a photoprotective cellular response. CarH activity as a transcription factor relies on the modulation of its oligomeric state by 5′-deoxyadenosylcobalamin and light. This review surveys current knowledge about these B_{12}-dependent photoreceptors, their distribution and mode of action, and the structural and photochemical basis of how they orchestrate signal transduction and control gene expression.

Contents

INTRODUCTION: LIGHT AND PHOTORECEPTORS

Sunlight is essential for life on Earth. Conversion of the energy contained in sunlight into chemical energy by photosynthetic bacteria, algae, and plants accounts for the majority of fixed biomass and molecular oxygen (1). A crucial environmental factor, the ability to sense and respond to light is vital for most living organisms. Human vision is based on the eye detecting visible light (or simply light), which corresponds to the 380–760 nm wavelength range of the electromagnetic spectrum (2, 3). Light can directly or indirectly signal diverse biological processes, including DNA repair, circadian rhythms, taxis, development, morphology, physiology, and virulence, and also mediate biosynthetic reactions, for example, in vitamin D_3 synthesis (4–13). The pervasive role of light in biology, however, comes with a price: Light absorption by photosensitive biomolecules like porphyrins, chlorophyll, or flavins can generate highly reactive oxygen species (ROS) that cause photooxidative damage of DNA, proteins, membranes, and other cellular components, and UV light triggers formation of mutagenic thymidine dimer lesions in DNA (14–18). Consequently, various cellular strategies have evolved to avoid, minimize, or repair light-induced damage (11, 14–16, 19).

Photoreceptors: proteins that sense light via a chromophore, which undergoes photochemical transformation and triggers conformational changes in the protein

Light, beneficial or harmful, has to be detected and converted to a cellular signal to elicit the appropriate response. In all domains of life, this fundamental task is carried out by photoreceptor proteins (or photoreceptors) that directly sense light through a chromophore component. For example, specific tryptophans in the UVR8 (UV resistance locus 8) protein sense UV light (20, 21). Visible light photoreceptors, however, must rely on noncovalently or covalently associated nonprotein chromophores, because no protein component absorbs in this wavelength range. Known chromophores include retinal, flavin mononucleotide (FMN), flavin adenine dinucleotide (FAD), *p*-coumaric acid (4-hydroxycinnamic acid), and 3′-hydroxyechinenone ketocarotenoid, all of which absorb in the blue-green region (2, 3, 6, 22–28), and linear tetrapyrroles (biliverdins,

phycocyanobilin, phytochromobilin, and phycoviolobilin), which absorb red/far-red light (29, 30). These unsaturated molecules have a conjugated π system with delocalized electrons, which favors light absorption (31). This type of system enables electron transfer, *cis–trans* isomerization about double bonds, or covalent bond formation–disruption to alter chromophore conformation and chemistry, which are then transmitted to the protein part of the photoreceptor to modulate function.

Optogenetics: a technology that combines genetic and optical methods to achieve rapid and precise control of biological processes

Photoreceptors have been classified into distinct families on the basis of the chromophore and protein sequence/structure conservation: Rhodopsins have retinal as chromophore; cryptochromes, LOV (light-oxygen-voltage), and BLUF (blue-light utilizing FAD) sensors use FMN or FAD; phytochromes rely on linear tetrapyrroles; xanthopsins employ *p*-coumaric acid; and orange carotenoid proteins have ketocarotenoid (12, 26, 28, 31, 32). Photoreceptors can be standalone proteins or part of larger proteins with multiple domains, each endowed with a defined activity, such as directing specific interactions (with proteins, DNA, RNA, membranes, small molecules) or enzymatic catalysis (kinases, diguanylate cyclases, phosphodiesterases). In multidomain photoreceptors, one or more modules sense the light input, undergo molecular changes, and transmit the signal to output effector domains to carry out a specific light-dependent function. The photosensory module frequently is an autonomous unit that can be swapped between different proteins, as is exemplified by the natural occurrence of a given type of photoreceptor module in functionally distinct proteins. In nature, this modularity allows for combinatorial module mixing as an effective strategy in the evolution of signaling and regulatory complexity (33). Biological engineers have also harnessed this modularity and created artificial genetic fusions of specific photoreceptor modules and proteins of interest, whose functions can then be optically monitored or controlled with high temporal and spatial precision (32). These advances have led to the vibrant field of optogenetics and the development of powerful tools and applications in cell biology and neurobiology (34–36).

The recent discovery of photoreceptors with a novel light-sensing chromophore, the vitamin B_{12} derivative 5′-deoxyadenosylcobalamin (simply, adenosylcobalamin or AdoCbl), has enlarged the number of known photoreceptor families and unveiled a new biological facet of this vitamin (37). Significant progress has been achieved in understanding how this new type of photoreceptor works. High-resolution structures of the functionally relevant states have revealed the molecular architecture of the photoreceptor and provided detailed snapshots of its light-dependent mechanism of action (38). Some fascinating features in the photochemistry have also been observed (39, 40). These aspects are covered here together with an overview of the discovery, functions, distribution, and evolution of these B_{12}-dependent photoreceptors.

VITAMIN B_{12}: CHEMISTRY AND BIOLOGY

Cobalamin Forms and Chemistry

Since its first discovery as the antipernicious anemia factor (41, 42), vitamin B_{12} has seen a rich and storied scientific history. A decade after its first isolation in 1948 (43, 44), the description of its crystal structure by Hodgkin et al. (45) marked a heroic moment for small-molecule crystallography, revealing one of nature's most complex cofactors in three dimensions, and its total chemical synthesis in the early 1970s capped a classic effort by Woodward, Eschenmoser, and coworkers (46). In parallel, extensive studies into the chemistry and biology of vitamin B_{12} and its derivatives, collectively referred to as the cobalamins or often just B_{12}, revealed their intricate chemical structure, complex reactivity, and rich spectroscopic properties as well as their biosynthetic origins and roles in living systems (47–52). Their best-characterized biological functions

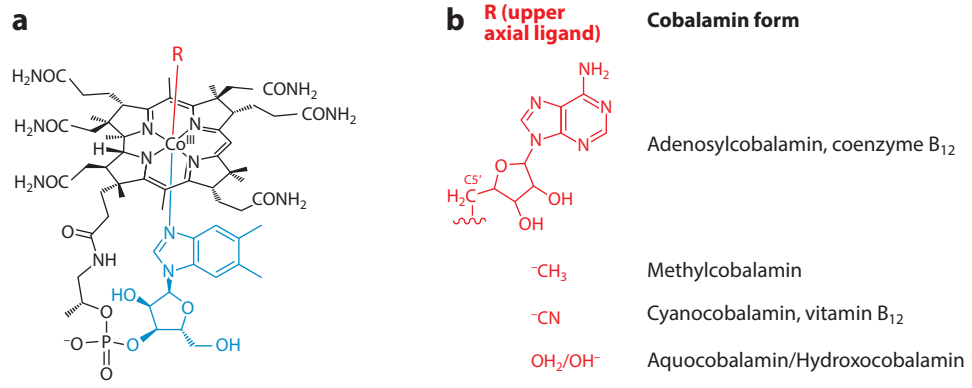

Figure 1

Vitamin B_{12} and derivatives. (*a*) General chemical structure of B_{12} in the base-on conformation with cobalt formally in the Co(III) state, the lower axial dimethylbenzimidazole ligand in blue, and the upper axial ligand denoted by R in red. (*b*) Selected upper axial ligands and the corresponding B_{12} forms are shown.

in fatty acid and folate metabolism make them essential micronutrients for humans and other animals, although curiously not for plants or fungi. Fitting for B_{12}'s storied history, more recent studies have revealed new and unanticipated biological functions, for example, in modulating the structure of microbial communities (53) and as a light sensor in light-dependent gene regulation, the main focus of this review.

Chemically, the principal feature of B_{12} is its corrin ring, whose four pyrrolic nitrogens coordinate a central cobalt atom that is usually in the Co^{3+} or Co(III) oxidation state. The corrin pyrroline and pyrrolidine groups are adorned with methyl, acetamide, and propionamide groups, one of which links the ring to the 5,6-dimethylbenzimidazole (DMB) ribonucleoside tail, characteristic of B_{12} (**Figure 1**). In free B_{12} at physiological pH, a nitrogen of this DMB base occupies the lower, or α, axial coordination site on the central cobalt, a conformation described as base-on or DMB-on. The octahedral coordination sphere of Co(III) is completed by an upper, or β, axial ligand, which can take a variety of forms depending on the B_{12} derivative (**Figure 1**).

The two major biological forms of B_{12}, methylcobalamin (MeCbl) and AdoCbl (also known as coenzyme B_{12}), both have an alkyl group as the upper axial ligand: MeCbl has a methyl group (Me) and AdoCbl has a 5′-deoxyadenosyl group (Ado) that is bonded to the cobalt through its 5′-carbon (**Figure 1**) (54, 55). Thus, both MeCbl and AdoCbl feature a covalent Co–C bond, as revealed by their respective structures (56, 57), and represent rare examples of naturally occurring organometallic compounds. Not surprisingly, these Co–C bonds have intriguing chemical properties: Chemically inert in the absence of light, their relatively low bond dissociation energies [reported as 32–40 kcal mol^{-1} for MeCbl and 24–35 kcal mol^{-1} for AdoCbl (58–62)] allow them to be cleaved rather easily. This feature underlies the use of MeCbl and AdoCbl as cofactors in enzyme catalysis, although their exact chemical properties and biological functions are distinct. Other B_{12} forms with different upper axial ligands are known (**Figure 1**). Cyanocobalamin (CNCbl or vitamin B_{12}) with a cyanide upper axial ligand is frequently found free in nature but is nonfunctional and has to be converted in vivo to MeCbl or AdoCbl for biological use. In the absence of other ligands, B_{12} in aqueous solution ligates a water molecule to form hydroxocobalamin or aquocobalamin (AqCbl), which predominates at physiological pH. Regardless of the upper axial ligand, free B_{12} forms are generally found in the DMB-on conformation at physiological pH. Protonation of DMB at low pH leads to its replacement by water, yielding the base-off (DMB-off)

conformation and a less rigid B_{12} molecule with altered chemistry (63). Various proteins, including the B_{12}-dependent photoreceptors reviewed here and many B_{12}-using enzymes, bind B_{12} with a His side chain replacing the DMB ligand, a B_{12}-binding mode known as base-off/His-on (64).

Under aerobic conditions, the central cobalt of the various B_{12} forms is generally in the +3 oxidation state and relatively redox inactive. Homolytic or heterolytic cleavage of the β-axial bond or reduction of AqCbl with a strong reductant can transiently generate cobalt in the Co^{2+}/Co(II) or Co^{1+}/Co(I) states, the coordination number decreasing from 6 in Co(III) to 5 in Co(II) and 4 in Co(I). The one-electron-reduced Co(II) form of B_{12}, termed cob(II)alamin or cob(II), is paramagnetic and can be detected by electron paramagnetic resonance (EPR) spectroscopy. This form is relatively inert under anaerobic conditions but rapidly oxidizes in the presence of molecular oxygen. Reduction by an additional electron to Co(I) yields cob(I)alamin or cob(I), a supernucleophile and potent reductant that decomposes even under anaerobic conditions. The unique chemical properties of B_{12} in each oxidation state are harnessed in various ways by different B_{12}-dependent enzymes.

Cobalamin Photochemistry

Cobalamins exhibit vibrant colors that originate from strong absorption in the UV–visible range, mostly from π–π^* transitions. The spectral features of each form depend on the cobalt oxidation state and the nature of the upper and lower axial ligands (65–67). As a result of this absorption, cobalamins exhibit rich and complex photochemistry, which is again modulated by the axial ligands (61, 62). Although the photochemical properties of CNCbl and AqCbl have been studied (68, 69), the discussion here centers on the biologically relevant alkylcobalamins MeCbl and AdoCbl, whose light sensitivity has been known since their first isolation. In particular, photolytic cleavage of the AdoCbl Co–C bond has been regarded as a model system for its cleavage in enzyme active sites (70) and therefore has been studied extensively. Early studies focused on determining the products of light-induced decomposition (70–73). The underlying photochemical processes are controlled by electronic relaxation dynamics that occur on picosecond timescales. Paired ultrafast transient absorption spectroscopy and theoretical calculations have emerged as powerful approaches for the study of B_{12} photochemistry and have provided detailed insight into the electronic processes and the intermediates following excitation (62, 74–78). Near-UV and visible light of wavelengths $<$530 nm (photon energies $>$40 kcal mol^{-1}) cleave the Co–C bond of both MeCbl and AdoCbl on a timescale of 10–100 ps. The quantum yields for MeCbl Co–C photolysis are wavelength dependent, high at 400 nm but much lower at 522 nm, whereas near unit quantum yields are observed for AdoCbl throughout this wavelength range (61, 62). The initial cleavage events are generally homolytic, generating a caged alkyl radical:cob(II) pair that can either recombine to regenerate the Co–C bond or dissociate. Competition between geminate recombination and radical escape determines the ultimate photolysis yield (79). Net photolysis is reduced by solvent cage effects around Cbl and accelerated by compounds such as molecular oxygen that can intercept the radicals formed and suppress recombination pathways (74, 80).

The fates of the alkyl radical and cob(II) generated upon photolysis of alkylcobalamins depend on the environmental conditions. In the case of MeCbl, the highly reactive methyl radical rapidly reacts through complex pathways to form formaldehyde and smaller amounts of methanol, formic acid, and carbon dioxide under aerobic conditions, and under anaerobic conditions it forms a mixture of formaldehyde, methane, and ethane, as well as smaller amounts of methanol and formic acid (72). Upon AdoCbl photolysis, the 5′-deoxyadenosyl radical (Ado$^\bullet$) rapidly reacts in the presence of molecular oxygen to form 5′-peroxyadenosine, which in turn decomposes to adenosine-5′-aldehyde and minor amounts of adenosine and adenine (39, 70). In the absence of

oxygen, Ado• undergoes intramolecular addition of the radical to the adenine base and forms 5′-deoxy-5′,8-cycloadenosine (71, 73). The second major photolysis product of both MeCbl and AdoCbl, cob(II), is stable under anaerobic conditions but is rapidly oxidized in the presence of oxygen to AqCbl, a reaction further enhanced by 5′-peroxyadenosine (70). The reactivity of these photolysis products underscores a central dichotomy of B_{12} biology: Although AdoCbl and MeCbl can mediate unique chemistry, their light sensitivity and reactivity require exquisite control to suppress inadvertent side reactions.

Cobalamins as Cofactors in Enzymes and Riboswitches

Although B_{12} is essential in animals and in many prokaryotes, only some of the latter can synthesize it de novo (51, 52). Plants, fungi, and many prokaryotes bypass the need for B_{12} by using only alternative enzymes or metabolic pathways that do not require this cofactor, and many other species contain both B_{12}-dependent and B_{12}-independent enzymes for the same reaction (48). Not surprisingly for such a complex molecule, the two B_{12} biosynthetic pathways (aerobic or anaerobic) are among the most intricate known in nature. Each pathway involves more than 30 genes and steps subject to genetic and enzymatic controls. The earliest steps lead to the formation of a tetrapyrrole precursor, uroporphyrinogen III, which is also common to heme and chlorophyll biosynthesis (48, 50, 81–84). The two B_{12} biosynthetic pathways then diverge, using different routes to convert the precursor into cobyrinic acid *a*,*c*-diamide, at which point they converge again to generate the B_{12} corrin ring and to attach the DMB. Given the high genetic and metabolic cost, organisms that require B_{12}, even ones capable of its biosynthesis, have evolved mechanisms to acquire and assimilate trace amounts of exogenous B_{12} and to salvage and regenerate the intracellular pool of this valuable cofactor (48, 85–89). Generally, external B_{12} in diverse forms (including ones lacking DMB, the cobinamides) is captured and transported into cells using dedicated proteins and sophisticated mechanisms in bacteria and animals. In the cell, imported B_{12} is usually processed (e.g., decyanation of CNCbl, dealkylation) by specialized enzymes and escorted with the aid of chaperones (to prevent side reactions and dilution) to the AdoCbl or MeCbl generation/utilization pathways (48, 85–90). MeCbl is directly produced and used by methionine synthase/methyltransferase; AdoCbl is produced by adenosine triphosphate–dependent adenosyltransferases (ATRs) for use by other factors (86, 89, 91, 92). Three classes of sequence-unrelated ATRs are known in bacteria: CobA (BtuR or CobO), which acts in de novo AdoCbl biosynthesis, and EutT and PduO, which convert imported B_{12} to AdoCbl (89, 92). The most widely prevalent and studied is PduO, whose human ortholog (MMAB) is associated with mitochondrial B_{12} metabolism (89).

B_{12}-dependent enzymes have been extensively surveyed elsewhere (54, 55, 63, 93–97), but a few aspects relevant to the theme of this review are highlighted here. B_{12} is used for three major types of reactions in biology: MeCbl is used for methyl transfer reactions; AdoCbl is used for radical-based transformations in mutases, dehydratases, deaminases, and class II ribonucleotide reductases; and cobalamin without an upper ligand is used by reductive dehalogenases and by the transfer RNA–modifying enzyme epoxyqueuosine reductase, whose structures and mechanisms have only started to emerge (98–101). The activities of these enzymes, which bind to their cofactor with K_D in the nM–mM range (97), are based on Co–C bond cleavage and formation of highly reactive species. The modes of Co–C bond cleavage and the resulting reaction mechanisms, however, are very distinct.

MeCbl-dependent enzymes catalyze heterolytic cleavage of the Co–C bond to form highly reactive cob(I), which retains both bonding electrons, and a methyl carbocation that is transferred to a nucleophilic acceptor. The prototypical member of this class, MeCbl-binding methionine synthase (termed MetH in bacteria), catalyzes transfer of a methyl group from 5-methyltetrahydrofolate

(MeTHF) to homocysteine (Hcy) for methionine synthesis (54, 55). This large monomeric enzyme has four structurally and functionally distinct domains, one each to bind Hcy, MeTHF, B_{12}, and *S*-adenosylmethionine (102). The crystal structure of its isolated MeCbl-binding domain provided the first visualization of B_{12} bound to a protein and of the base-off/His-on B_{12}-binding mode (64), which has since been observed in many other B_{12}-dependent enzymes. Structural and biochemical studies have provided a framework to understand the workings of this enzyme and the mechanistic safeguards that protect the reactive MeCbl cofactor (55, 103). MeCbl is sandwiched between a Rossmann-fold domain, which binds the B_{12} lower face and the DMB tail, and a four-helix bundle, which caps the B_{12} upper face and prevents inadvertent loss of the methyl group (64, 104). Thus, MeCbl is sequestered, requiring that the MeTHF- and the Hcy-binding domains of MetH displace the four-helix bundle to gain access during catalysis (55, 103).

In the presence of the corresponding substrate, AdoCbl-dependent enzymes catalyze homolytic cleavage of the AdoCbl Co–C bond to generate cob(II) and Ado$^\bullet$, which initiates a chemical transformation by abstracting a hydrogen atom from the substrate (93). At the end of the catalytic cycle, Ado$^\bullet$ is regenerated and recombines with cob(II) to restore AdoCbl for another round of catalysis. AdoCbl is thus a radical reservoir in AdoCbl-dependent enzymes, allowing for reversible access to the working species, Ado$^\bullet$, as required. Examples of these enzymes include methylmalonyl–coenzyme A mutase and its relatives, which interconvert branched and linear acyl groups through carbon skeleton transformations; aminomutases, which migrate the terminal amino groups of lysine or ornithine; and eliminases, which mediate migration and elimination of a hydroxyl or amino group. Not surprisingly, these radical-based reactions must take place under carefully controlled conditions to prevent side reactions and oxidative quenching of intermediates. To achieve these conditions, AdoCbl-dependent enzymes bind AdoCbl in a buried cavity between two domains: a substrate-binding domain, usually an $(\alpha/\beta)_8$ triose phosphate isomerase barrel, and a B_{12}-binding domain that is either a Rossmann-fold domain homologous to that in MetH or a distinct domain that binds AdoCbl base-on (93). In this architectural context, Ado$^\bullet$ generation and the ensuing chemical transformations occur in a controlled environment, thereby enabling the difficult radical-based chemistry of AdoCbl-dependent enzymes.

Beyond its function as an enzyme cofactor, B_{12} can also bind to RNA-based regulatory elements termed riboswitches (105, 106) (see the sidebar titled Riboswitches). The first such RNA element to be discovered, the AdoCbl riboswitch, spans the $\geq$200 nt 5′ untranslated region of mRNA from genes involved in B_{12} metabolism (105, 107). Both the AdoCbl and the more recently discovered AqCbl riboswitches bind tightly ($K_D \approx$ 10–250 nM) to the respective base-on B_{12} form using similar RNA structural cores, with additional peripheral extensions in the AdoCbl riboswitch conferring cofactor specificity (108, 109). The less common AqCbl riboswitch was speculated to have evolved in marine bacteria owing to their high light exposure, which would favor greater availability of AqCbl over the less light-stable AdoCbl (108). However, the photochemistry and photobiology of these B_{12} riboswitches remain unexplored. Interestingly, B_{12} riboswitches typically

RIBOSWITCHES

These RNA-based elements, found mostly in bacteria and archaea (and a few plants), mediate a mode of gene regulation based on RNA conformational changes upon binding to ligands like vitamins, amino acids, nucleotides, aminosugars, or metals. Riboswitches can regulate transcription or translation and generally act in *cis*, although some that act in *trans* are also known. The first discovered riboswitch and the second-most widespread is the AdoCbl riboswitch.

sense the presence of AdoCbl (or AqCbl) to regulate expression of proteins involved in B_{12} uptake, biosynthesis, or use, whereas the photoreceptors reviewed here sense a light-dependent change in the state of B_{12} to control expression of genes apparently unrelated to B_{12} metabolism.

DISCOVERY OF CarA AND CarH, AND A ROLE FOR VITAMIN B_{12} IN LIGHT RESPONSE

Even though the light sensitivity of AdoCbl and MeCbl was known for years, this property was thought to serve no physiological function. The light sensitivity is actually undesired in enzyme catalysis, as it leads to cofactor inactivation. The discovery that B_{12}, specifically AdoCbl, can serve as a light sensor thus represented a major surprise. This new facet of B_{12} biology emerged from studies in the gram-negative soil bacterium *Myxococcus xanthus*, in which light induces a transcriptional response leading to carotenoid biosynthesis (11, 110). Carotenoids protect cells against photooxidative damage by quenching singlet oxygen ($^1O_2$) and other ROS (14, 16, 110, 111), and light has been shown to generate $^1O_2$ and trigger the response in *M. xanthus* (112). Yet, despite its well-established light response, genetic and bioinformatic studies have failed to identify conventional photoreceptors in *M. xanthus* (11).

A resolution to this conundrum and the earliest hints for a role of B_{12} in a cellular response to light came from the identification of the first putative B_{12}-binding transcription factors: the paralogous *M. xanthus* repressors of carotenoid (*car*) gene expression CarA and CarH, encoded by the two most downstream genes of the light-inducible *carB* operon, which groups all but one of the structural genes for carotenoid biosynthesis (**Figure 2**) (11, 110, 113). Their N-terminal sequences resembled the DNA-binding domain (DBD) of MerR (mercury-sensing regulator) family transcription factors (**Figure 2*b***) (113–118), suggesting a direct involvement in regulating gene expression (118) (see the sidebar titled MerR Protein Family). Their C-terminal segments were noteworthy, as they resembled the MeCbl-binding domain of MetH in sequence, size, and predicted secondary structure and in having the base-off/His-on B_{12}-binding motif (**Figure 2*b***) (113), first described by Drennan et al. (64) and originally found only in enzymes that use B_{12} as a cofactor. As predicted, CarA did bind to B_{12} but, paradoxically, functioned independently of the cofactor. Whether or not B_{12} was present, CarA could bind to DNA using its autonomous, N-terminal MerR-type DBD (119, 120) and dimerize via its C-terminal module (37, 121, 122). To repress transcription, the CarA dimer appears to bind to a bipartite operator in a stepwise cooperative manner, first to a high-affinity palindrome and then to a second similar but lower-affinity one downstream, which overlaps with the −35 element of the promoter (P_B) of the *carB* operon, to block RNA polymerase access to P_B (**Figures 2*a*** and **3*a***) (123). Light abolishes CarA-mediated repression by inducing expression of CarS, an antirepressor that structurally mimics operator DNA to bind tightly to the CarA DNA recognition helix and physically sequester it from operator binding (**Figure 3*a***) (122–125).

MerR PROTEIN FAMILY

The MerR (mercury-sensing regulator) family of transcription factors regulates responses to heavy metals, drugs, and other stresses in bacteria. They are dual-function regulators that can repress or activate a promoter by binding as dimers to a site with (pseudo)palindromic sequences, which is located within a spacer of suboptimal length between the −10 and −35 promoter elements.

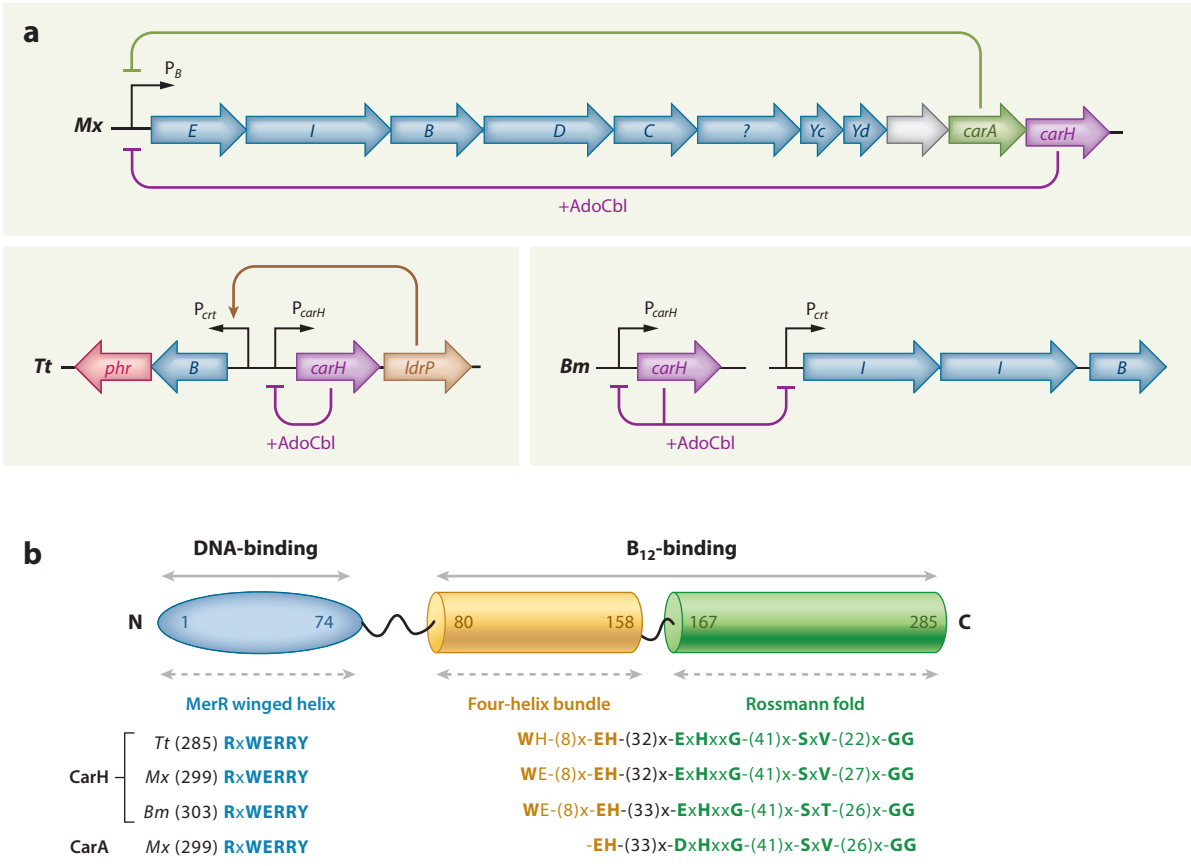

Figure 2

Experimentally studied CarH and CarA proteins. (*a*) Genomic context of the *carH/carA* genes in *Myxococcus xanthus* (*Mx*), *Thermus thermophilus* (*Tt*), and *Bacillus megaterium* (*Bm*). Other genes and their corresponding products are as follows: *crtE* (*E*), farnesyltransferase; *crtI* (*I*), phytoene desaturase; *crtB* (*B*), phytoene synthase; *crtD* (*D*), hydroxyneurosporene dehydrogenase; *crtC* (*C*), neurosporene hydroxylase; *?*, putative carotenoid biosynthesis protein; *crtYc* (*Yc*) and *crtYd* (*Yd*), components of a heterodimeric lycopene cyclase; white arrow, predicted acyltransferase domain-containing protein; *phr*, DNA photolyase; *ldrP*, CRP/FNR family transcriptional regulator. Carotenoid synthesis genes are shown in blue. (*b*) Domain architecture of CarH/CarA proteins. Numbers delimiting the domains are from the crystal structure of CarH from *Tt*. Characteristic motifs (x, any residue) are shown below for each protein (size in residues is indicated in parentheses). Abbreviations: AdoCbl, 5′-deoxyadenosylcobalamin; CarA, B_{12}-independent repressor of carotenogenesis; CarH, B_{12}-dependent repressor of carotenogenesis; CRP, cAMP receptor protein; FNR, fumarate and nitrate reductase; MerR, mercury-sensing regulator; P_B, promoter of the *carB* operon; P_{carH}, promoter of the *carH* gene; P_{crt}, promoter of carotenogenic gene(s).

Repression of P_B in the dark was abolished on deleting *carA*, but intriguingly, it was restored on supplying B_{12} exogenously (*M. xanthus* cannot synthesize B_{12} de novo but has the cellular machinery for its uptake and assimilation) as long as the CarA operator was intact (113, 121). Detailed genetic analysis in a *carA*-deleted genetic background demonstrated that downregulation of P_B by B_{12} required CarH and its B_{12}-binding motif (121). These findings thus revealed that light-induced carotenogenesis in *M. xanthus* was regulated by two parallel and distinct pathways orchestrated by a pair of paralogous factors, of which one (CarH), but not the other (CarA), required vitamin B_{12} (121). The study also established a firm link between B_{12} (the form used was

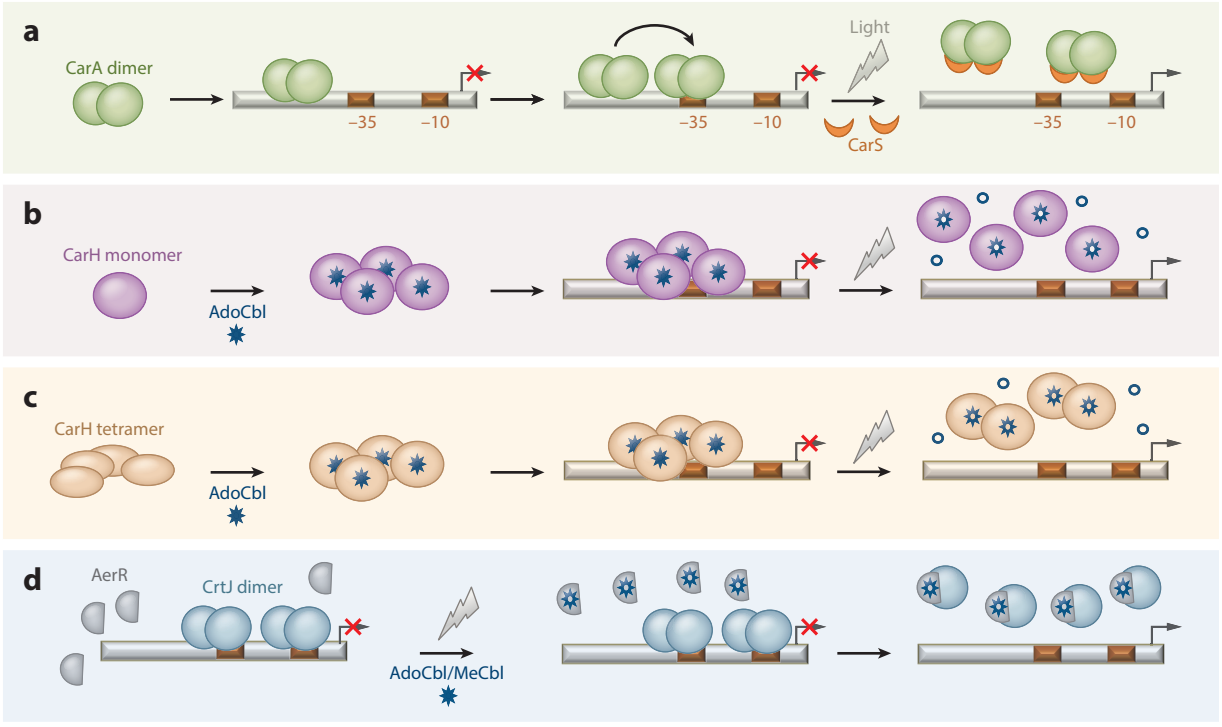

Figure 3

Light-dependent gene regulation mechanisms by B_{12}-binding transcription factors. (*a*) *Myxococcus xanthus* CarA and CarS. Cooperative binding of CarA dimers to a bipartite operator overlapping the −35 promoter region blocks access to RNA polymerase and represses transcription in the dark. Light induces production of CarS, which sequesters CarA, prevents operator DNA binding, and activates transcription. (*b*) *M. xanthus/Thermus thermophilus* CarH. CarH monomers in the apo form bind to AdoCbl (*filled blue asterisk*) to form stable AdoCbl-bound CarH tetramers in the dark, which bind to operator DNA overlapping the −35 promoter region to block access to RNA polymerase and repress transcription. Light disrupts AdoCbl–CarH tetramers to monomers by photolysis of bound AdoCbl (*unfilled blue asterisks* and *blue circles* represent, respectively, photolyzed cobalamin and 4′,5′-anhydroadenosine, the latter experimentally demonstrated in *b* and expected in *c*), provoking loss of operator binding and activation of transcription. (*c*) *Bacillus megaterium* CarH. ApoCarH tetramers, which do not bind DNA, yield AdoCbl-bound tetramers that bind to operator DNA overlapping the −35 region of P_{carH} (another operator that overlaps the −10 region of P_{crt} is not shown) to repress transcription in the dark. Light disrupts AdoCbl–CarH tetramers to dimers by photolysis of bound AdoCbl, abolishing operator binding and relieving repression. (*d*) *Rhodobacter capsulatus* CrtJ and AerR. CrtJ dimers repress transcription in the dark by binding to two sites overlapping the −10 and −35 promoter regions. On exposure to light, binding of AqCbl (produced by AdoCbl or MeCbl photolysis) to AerR enables its association with CrtJ to disrupt CrtJ dimers and DNA-binding, activating transcription. Abbreviations: AdoCbl, 5′-deoxyadenosylcobalamin; AerR, aerobic repressor of photosynthesis; AqCbl, aquocobalamin; CarA, B_{12}-independent repressor of carotenogenesis; CarH, B_{12}-dependent repressor of carotenogenesis; CarS, antirepressor of CarA; CrtJ, aerobic repressor of carotenoid (*crt*) gene expression; MeCbl, methylcobalamin; P_{carH}, promoter of the *carH* gene; P_{crt}, promoter of carotenogenic gene(s).

unknown at this point) and CarH in light-dependent gene regulation and marked the discovery of a role for B_{12} as a light sensor.

M. xanthus CarA and CarH were the only known transcription factors with a B_{12}-binding domain fused to a DBD until a later study reported a protein with a similar domain architecture acting in light-induced carotenogenesis in the gram-positive soil bacterium *Streptomyces coelicolor* (126). Molecular details on how this protein, named LitR (for light-induced transcription regulator), functions and whether or not it requires B_{12} remain unaddressed. The subsequent outpouring of microbial genome data revealed many bacterial species with genes for CarA/CarH homologs

of unknown function, often amid ones for carotenogenesis or light-related responses (37, 121). Studies of a selected few of these are now revealing the molecular basis for their distinct modes of action.

MOLECULAR MECHANISMS OF B_{12}-BASED PHOTORECEPTORS

Adenosylcobalamin in Light-Dependent Gene Regulation by CarH

The mechanistic basis for the combined action of CarH and B_{12}, the link to light, and the specific form of B_{12} involved emerged in a pioneering study reported in 2011 (37). Domain swap and bacterial two-hybrid analyses firmly established that the C-terminal domain of CarH conferred the B_{12} dependence in vivo, with B_{12} controlling the oligomeric state of this domain (37). In-depth analysis of the molecular interplay between CarH and B_{12} was, however, thwarted by the inability to purify native *M. xanthus* CarH. The existence of a homolog of unknown function in *Thermus thermophilus* (a gram-negative bacterium that can synthesize B_{12} de novo) enabled not only comparative studies but also, as it was easily purified, its biochemical, hydrodynamic, structural, and photochemical characterization (37–40, 127). The *T. thermophilus* protein and a chimera with its DBD replaced by that of *M. xanthus* CarH (which could functionally replace *M. xanthus* CarH in vivo) exhibited, in vitro, B_{12}-dependent oligomerization and DNA binding in the dark that was disrupted by light. Surprisingly, the form of B_{12} required turned out to be AdoCbl, despite the similarity of the CarH B_{12}-binding domain to that in MeCbl-dependent MetH (37). Only AdoCbl rapidly transformed the monomeric apoprotein into a stable tetramer that has 1:1 AdoCbl:CarH stoichiometry and binds tightly to operator DNA ($K_D \approx 70$ nM) (37, 38). Photolysis of AdoCbl–CarH by exposure to near-UV, blue, or green light swiftly provoked disassembly of the tetramer to monomers, with concomitant loss of operator binding (**Figure 3*b***) (37, 127). Interestingly, *T. thermophilus* CarH retains the photolysed AdoCbl as a stable adduct, refractory to exchange with fresh AdoCbl (38, 40). That AdoCbl is also the B_{12} form required by *M. xanthus* CarH was evident when the deletion of the only gene encoding an ATR (of the PduO type) in this bacterium, which would cause an abrogation of intracellular AdoCbl generation, resulted in the loss of B_{12}-dependent repression of carotenogenesis. Moreover, even in the absence of the CarS antirepressor, light still relieved repression by *M. xanthus* CarH. These studies thus established that *M. xanthus* CarH also directly senses light using AdoCbl to regulate gene expression (37).

The location of the gene for *T. thermophilus* CarH next to one for carotenogenesis, as in *M. xanthus* (**Figure 2*a***), suggested a function in light-regulated carotenoid synthesis, which was indeed demonstrated (128). However, although *M. xanthus* CarH acts at a promoter that drives expression of the genes for carotenoid synthesis as well as its own, the one in *T. thermophilus* represses its own promoter and that of LdrP, a transcriptional activator of the carotenogenic gene transcribed in the opposite direction (**Figure 2*a***) (128). In another variation recently found in *Bacillus megaterium* (a gram-positive bacterium that can synthesize B_{12} de novo), the CarH homolog regulates its own expression and that of target carotenogenic genes present at an unlinked genetic locus (**Figure 2*a***) (129). Here, the active dark-state AdoCbl-bound repressor is again a tetramer, but its inactivation by light yields a dimer rather than a monomer (**Figure 3*c***) (129).

Another Mode of Gene Regulation Dependent on B_{12} and Light: AerR

A new twist to B_{12}-dependent light-regulated gene expression was reported with AerR (aerobic repressor of photosynthesis), a small, stand-alone B_{12}-binding protein found in *Rhodobacter capsulatus* and related α-proteobacteria (130, 131). AerR (also termed PpaA) is an antirepressor of CrtJ

[the aerobic repressor of carotenoid (*crt*) gene expression; also termed PpsR], a dimeric, redox-regulated repressor of genes for carotenoid, heme, and bacteriochlorophyll biosynthesis and for structural proteins of the light-harvesting complex II (130, 132, 133). Like CarA, the CrtJ dimer binds cooperatively to two tandem palindromes in the promoter region to repress transcription and requires an antirepressor (AerR) for derepression in the light (132). But unlike the CarA antirepressor CarS, AerR is not transcriptionally activated by light but instead binds to AqCbl, which is produced in the light by photolysis of AdoCbl (or MeCbl). AqCbl-bound AerR then targets CrtJ to disrupt its oligomerization, DNA binding, and repressor activity (**Figure 3*d***) (130, 131). As in *T. thermophilus* CarH, photolysed B_{12} is tightly bound to AerR. Two His in AerR were implicated in this tight binding, one corresponding to the base-off/His-on B_{12}-binding motif and another that is not conserved in its homologs (130).

The CarH Tetramer: Structural Comparisons with Known DNA- and B_{12}-Binding Proteins

A series of crystal structures of the functionally relevant states of *T. thermophilus* CarH and structure-based mutational analysis by our groups recently provided detailed insight into the architecture and the light-dependent conformational changes of the CarH photoreceptor (38). The dark AdoCbl–CarH tetramer is a dimer of two dimers, each with a striking head-to-tail arrangement of two monomers. The N-terminal domain of each monomer structurally matches the winged-helix DBD found in CarA (**Figure 4*a***) (119) and MerR-type transcription factors (114–116). It has the canonical DNA recognition α-helix, with a conserved RxWERRY motif in CarH, its homologs, and CarA (**Figure 2*b***), and the β-hairpin wing. The CarH DBD conserves most of the residues that contact DNA in CarA (119) and in MerR proteins (114–116) but employs a distinct DNA-binding mode described in the next section. The DBD adopts different orientations relative to the C-terminal domain owing to a flexible linker of ∼6 residues observed in the *T. thermophilus* CarH structure. Remarkably, the C-terminal AdoCbl-bound light-sensing module is structurally more similar to the MetH MeCbl-binding domain (64) than to any known AdoCbl-binding protein (**Figure 4*a***). As in MetH, this CarH module has a four-helix bundle, which contacts the upper face of the Cbl, followed by a five-stranded α/β Rossmann domain that binds the lower face in the base-off/His-on mode using the conserved His of the Glu/Asp-x-His or E/DxH (where x is any residue) B_{12}-binding motif (**Figures 2*b*** and **4*a***). But in contrast to the

Figure 4

Dark-state AdoCbl-bound CarH compared with structurally similar DNA- and B_{12}-binding domains. (*a*) CarH protomer structure (PDB accession code 5C8D) showing the modules for DNA binding (compared with that in CarA, *top left*; PDB accession code 2JML) and B_{12} binding (compared with that in MetH, *bottom left*; PDB accession code 1BMT). (*b*) Close-up of the B_{12} binding site showing residues contacting the upper axial ligand (*cyan*) of MeCbl in MetH and cobalt-coordinating His (H759). (*c*) Close-up of the B_{12} binding site showing residues contacting the upper axial ligand (*cyan*) of AdoCbl in CarH and cobalt-coordinating His (H177). For a better view, the orientation in panels *b* and *c* is slightly different from that in panel *a*. (*d*) Comparison (in stereo) of the orientations of the AdoCbl Ado group in CarH, in free AdoCbl, and in selected enzymes whose structures have been determined with intact AdoCbl, IcmF (PDB accession code 4XC6) and related mutases, and OAM in its resting state (PDB accession code 3KP1). Abbreviations: AdoCbl, 5′-deoxyadenosylcobalamin; CarA, B_{12}-independent repressor of carotenogenesis; CarH, B_{12}-dependent repressor of carotenogenesis; IcmF, isobutyryl-coenzyme A mutase fused protein; MeCbl, methylcobalamin; MerR, mercury-sensing regulator; MetH, MeCbl-binding methionine synthase; OAM, ornithine-aminomutase; PDB, Protein Data Bank.

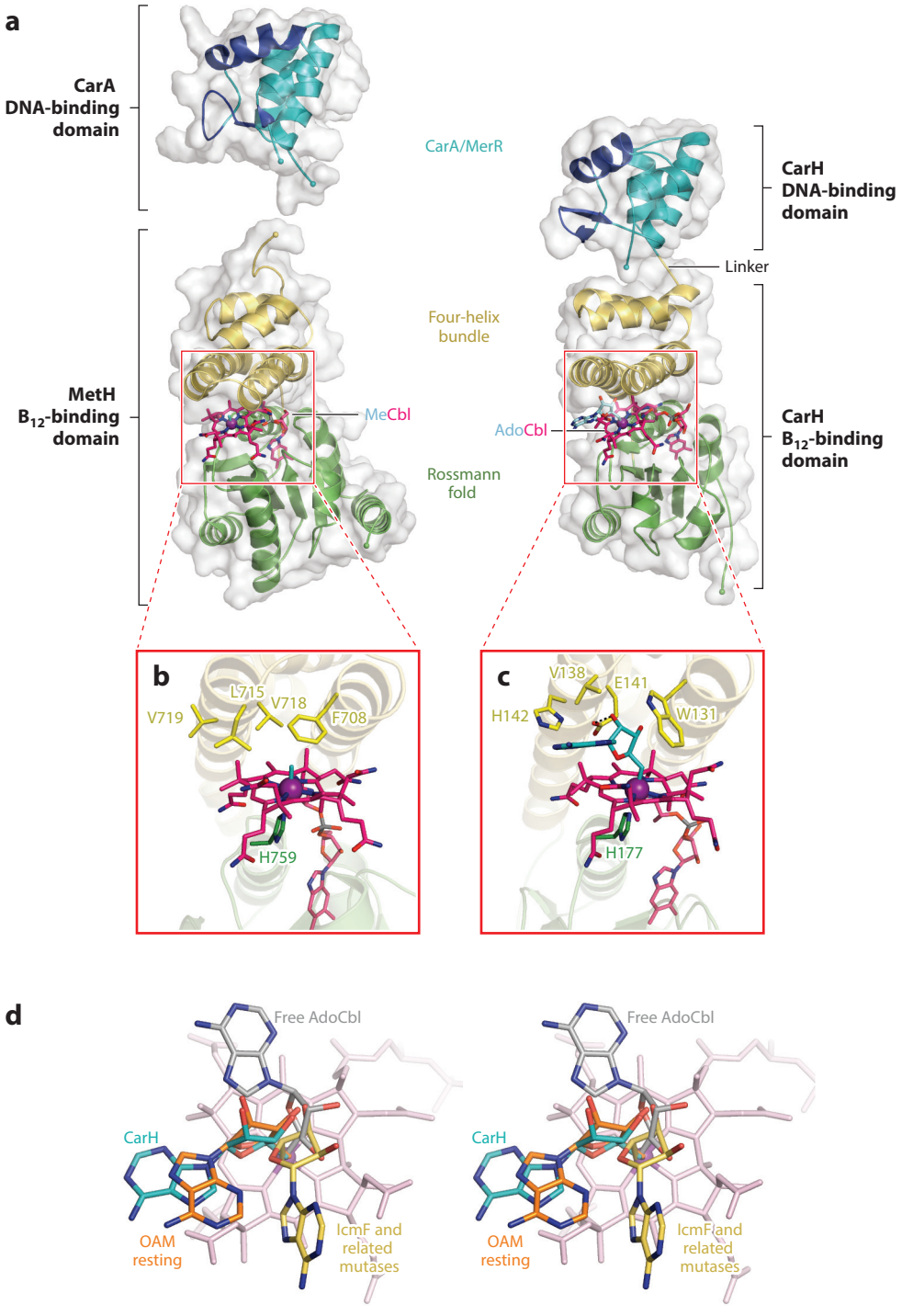
a
CarA DNA-binding domain
MetH B12-binding domain
MeCbl
CarA/MerR
CarH DNA-binding domain
Linker
Four-helix bundle
AdoCbl
CarH B12-binding domain
Rossmann fold
b
L715
V718
V719
F708
H759
c
V138
E141
H142
W131
H177
d
Free AdoCbl
CarH
OAM resting
IcmF and related mutases
Free AdoCbl
CarH
OAM resting
IcmF and related mutases

MetH module, in which only the Me of MeCbl can fit snugly as the upper axial ligand, the CarH B_{12} binding pocket accommodates the far bulkier Ado group of AdoCbl. Also, AdoCbl–CarH is a tetramer whose B_{12}-binding modules act as light sensors (37, 127), whereas the large multidomain MetH is a monomer (102) whose B_{12}-binding module suppresses undesired light-induced side reactions (104).

The CarH structure reveals how an enlarged B_{12} binding pocket and the substitution of four hydrophobic residues in the four-helix bundle, Phe708, Leu715, Val718, and Val719 in MetH to Trp131, Val138, Glu141, and His142, respectively, in CarH (**Figure 4*b*,*c***), allowed for the repurposing of the MetH MeCbl-binding module into one that binds AdoCbl (38). These changes produce a larger cavity, a more polar environment, and an H-bond between Glu141 and the Ado ribose group. Moreover, the Phe in MetH is directly above the Me group of MeCbl to protect it from photolysis (104), whereas the larger side chain of the equivalent Trp in CarH is to the side of the Ado group in AdoCbl, contacting its ribose moiety. Although the AdoCbl Co–C bond length in CarH (2.2 Å) (38) is similar to that in the free form or in the substrate-free resting state of AdoCbl-based enzymes (93), the relative orientation of the Ado group differs (**Figure 4*d***). Consistent with their importance, the aforementioned Trp, Glu, and His form a conserved W-(9)x-EH motif in CarH homologs, and mutating any of these residues impairs AdoCbl binding and tetramerization (38). Tellingly, *M. xanthus* CarA, which binds to B_{12} but does not require it for oligomerization or function (37), retains the Glu and His but lacks the Trp and four other adjacent residues (**Figure 2*b***).

The presence of the Ado group maintains the AdoCbl-bound protomer in an extended conformation, which allows the helix bundle of one monomer unit to pack against the Rossmann fold of another unit to form a head-to-tail dimer. The dimer interface between the head-to-tail monomeric units is extensive, with more than 20 H-bonds and salt bridges, some involving the Ado group (**Figure 5*a***). Tetramers form by packing two head-to-tail dimers in a staggered manner (**Figure 5*b***). Assembly of the tetramer from apoprotein monomers upon adding AdoCbl is so rapid and favorable that dimers are detected only if the dimer–dimer interface is disrupted by

Figure 5

The CarH tetramer and its unexpected DNA binding mode. (*a*) The head-to-tail packing of the two protomers in a CarH dimer is shown, with the helix bundle in yellow, the AdoCbl-binding domain in green, and the two DBDs in cyan. On the right is a close-up of the extensive interface of the head-to-tail dimer with several H-bonds and ionic interactions indicated. D201 and R176 indicate residues whose interaction was shown to be crucial by mutational analysis. (*b*) The CarH tetramer of two head-to-tail dimers is shown with the four DBDs (*purple*, *cyan*, *light cyan*, and *dark blue*) (PDB accession code 5C8D). Two alternative views of the tetramer are shown to better appreciate the complex quaternary structure of CarH. The view on the left shows the distribution of the DBDs on the protein surface (DBDs shown in *pink* and *dark blue* correspond to the head-to-tail dimer at the back, whose B_{12}-binding domains are shown in *gray*). (*c*) CarH tetramer (colored as in panel *b*) in complex with DNA (PDB accession code 5C8E) is shown. Three DBDs are reoriented and contact three DRs in the DNA sequence, depicted schematically below (structures in *b* and *c* are redrawn versions of those previously reported in Reference 38). (*d*) Direct repeats recognized by CarH at P_{carH} in *Tt* determined from the structure of the complex and those inferred in *Mx* and *Bm* from footprinting data and sequence inspection are shown. Base pairs covered by the recognition helix, as deduced from the CarH–DNA structure, are shaded. The −35 promoter region is shown in red. In *Mx* P_B, the two CarA binding site palindromes are underlined. The repeats in *Bm* P_{crt} and its −10 region (*purple*) correspond to the noncoding strand. The DNA sequence logo for a probable consensus CarH direct repeat recognition site from the sequences above is shown (*bottom*). Abbreviations: AdoCbl, 5′-deoxyadenosylcobalamin; *Bm*, *Bacillus megaterium*; CarH, B_{12}-dependent repressor of carotenogenesis; DBD, DNA-binding domain; DR, direct repeat; *Mx*, *Myxococcus xanthus*; P_B, promoter of the *carB* operon; P_{carH}, promoter of the *carH* gene; P_{crt}, promoter of carotenogenic gene(s); PDB, Protein Data Bank; *Tt*, *Thermus thermophilus*.

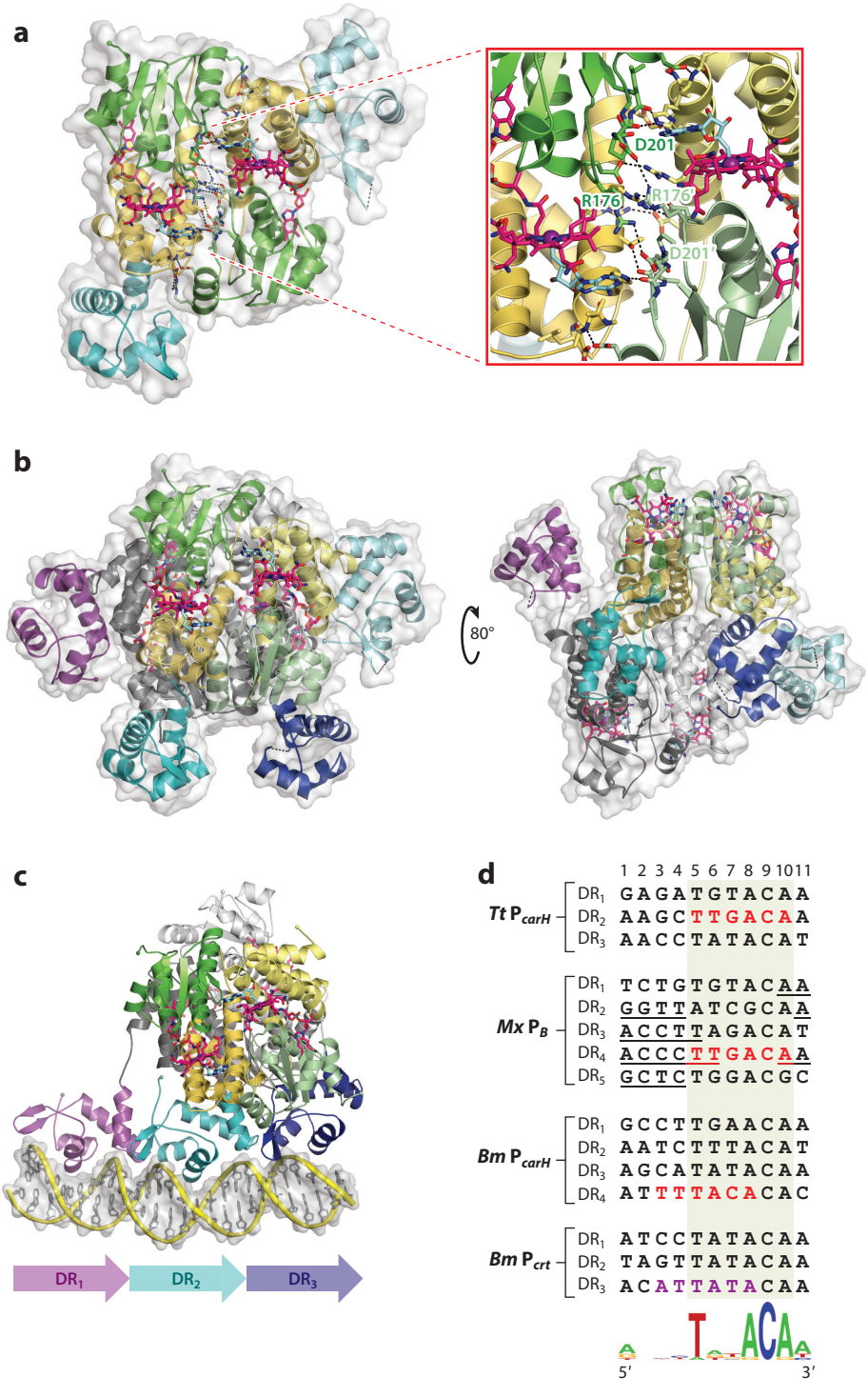
a
D201
R176
R176'
D201'
b
80°
c
DR1
DR2
DR3
d
1 2 3 4 5 6 7 8 9 10 11
Tt PcarH
DR1 G A G A T G T A C A A
DR2 A A G C T T G A C A A
DR3 A A C C T A T A C A T
Mx PB
DR1 T C T G T G T A C A A
DR2 G G T T A T C G C A A
DR3 A C C T T A G A C A T
DR4 A C C C T T G A C A A
DR5 G C T C T G G A C G C
Bm PcarH
DR1 G C C T T G A A C A A
DR2 A A T C T T T A C A T
DR3 A G C A T A T A C A A
DR4 A T T T T A C A C A C
Bm Pcrt
DR1 A T C C T A T A C A A
DR2 T A G T T A T A C A A
DR3 A C A T T A T A C A A
5′
3′

mutation (37, 38, 127). Residues at the dimer and tetramer interfaces are not highly conserved, but key interactions appear to be retained. For example, an Arg–Asp salt bridge between Arg176 in one monomer and Asp201 in the other is crucial for dimerization (**Figure 5*a***), as its disruption produces monomers, but can be swapped for an Asp–Arg or a Glu–Arg pair (38). In *M. xanthus* CarH, this pair is already swapped in the form of a Glu–Arg pair but is also indispensable for oligomerization and can be replaced by Arg–Glu in vivo (J. Fernández-Zapata, M.C. Polanco, S. Padmanabhan & M. Elías-Arnanz, unpublished findings). Intriguingly, CarA, unlike CarH, forms dimers independently of B_{12} or light (37), and some AdoCbl-dependent CarH homologs, such as that in *B. megaterium*, are active as repressors in the tetrameric form but become dimers instead of monomers in the light (**Figure 3**) (129). Structures of these homologs can provide insights into why their oligomerization behavior differs from that observed for *T. thermophilus* CarH.

CarH's architecture of a tetramer formed by two head-to-tail dimers is rather unusual for a transcription factor. This arrangement results in neighboring DBDs being pointed away from each other (**Figure 5*b***). Very few structures of transcription factors with such a head-to-tail assembly are known. One example, *Bacillus subtilis* GabR (γ-aminobutyric acid metabolism regulator), has an N-terminal winged-helix domain connected by a long, flexible, 29-residue linker to a C-terminal domain with an aminotransferase (AT) family fold that binds to pyridoxal 5′-phosphate (PLP), the vitamin B_6 coenzyme (134, 135). With or without bound PLP, two AT domains are packed head-to-tail to form a stable GabR dimer (134). The GabR–DNA complex structure is not known, but it has been proposed that a GabR dimer binds to two direct ATACCA repeats, separated by a 29 bp AT-rich spacer that is bent in the complex and includes the −35 promoter region (134, 135). The DNA-binding mode of CarH, however, is distinct.

The Surprising Mode of DNA Binding by CarH

The crystal structure of the CarH–DNA complex revealed a surprising mode of DNA binding, with three out of the four DBDs in the CarH tetramer contacting three adjacent sites (**Figure 5*c***). This binding mode was corroborated by hydroxyl radical footprinting and systematic analysis of CarH binding to mutant operators (38). The CarH tetramer, alone or DNA bound, has the same overall architecture except for a reorientation of three DBDs to contact three adjacent direct 11 bp repeats, the central one containing the TTGACA of the −35 promoter element (**Figure 5*c*,*d***) (38). H-bonds and electrostatic interactions position the recognition helix of each DBD (involving the conserved RxWERRY motif) in the major groove and the β-hairpin wing in the minor groove. Mutating DNA contacts in any two repeats or in all three, but not in just one, abolishes binding by CarH. Tight DNA binding requires a tetramer, because mutants that form only dimers bind DNA with reduced affinity and cooperativity, and light-induced monomers do so poorly (37, 38).

It is intriguing that the *T. thermophilus* CarH tetramer uses three out of four DBDs to contact three adjacent DNA sites and, accordingly, only three direct repeats can be identified in its operator segment (**Figure 5*d***) (38). Curiously, within the ∼50 bp *M. xanthus* CarH operator (which also spans that of CarA) mapped using the chimera with the *M. xanthus* CarH DBD fused to the *T. thermophilus* CarH AdoCbl-binding domain mentioned earlier (37), five direct repeats similar to those of *T. thermophilus* can be identified (**Figure 5*d***). Future studies will help establish the actual number of repeats and DBDs required for DNA binding and function in this case. Interestingly, AdoCbl-bound *B. megaterium* CarH has been reported to bind to two DNA sites located at unlinked genetic loci (**Figure 2*a***) (129). One DNA site overlaps with the −35 element of its own promoter (P_{carH}), and the other includes the −10 element of the promoter for the carotenogenic operon (P_{crt}); in both cases, an imperfect interrupted palindrome with two 6 bp half-sites separated by 16 bp was proposed as the binding site (129). However, four and three similar direct repeats

can be discerned in the P_{carH} and P_{crt} sites, respectively (**Figure 5*d***). Thus, the *B. megaterium* CarH tetramer could conceivably target direct repeats, as does *T. thermophilus* CarH, rather than a palindrome as proposed, although this possibility remains to be established experimentally. The activities of signaling proteins such as photoreceptors often dramatically depend on the properties of the linker between the receptor and effector modules (136). The intrinsically unstructured linker between the CarH DBD and the light-sensing oligomerization module, whose length and sequence vary in different homologs (~6 residues in *T. thermophilus*, ~20 in *M. xanthus*, ~14 in *B. megaterium*), could underlie a flexible DNA-binding mode of CarH, an aspect that needs to be explored. The finding that the *B. megaterium* homolog can bind to a site that overlaps with the −10 promoter element (**Figure 5*d***) suggests that CarH can target the −35 as well as the −10 promoter elements to achieve transcriptional repression. The CarH proteins that have been studied, although from distantly related bacteria, may nonetheless recognize similar 11 bp repeats, with highly conserved bases at positions 5 (T), 8 (A), 9 (C), and 10 (A) (**Figure 5*d***). Occurrence of these conserved bases in adjacent repeats could help identify other CarH-regulated promoters.

Interestingly, in binding as a tetramer to direct repeats, CarH conserves most of the DNA contacts of CarA and MerR proteins, even though the latter bind as dimers to (pseudo)palindromic sequences (114–117, 119, 123). But unlike MerR factors, CarH and CarA are known to repress transcription by binding to sites overlapping a promoter with optimal spacer length (38, 119, 121, 123). Whereas CarA does this as a dimer, and independently of B_{12}, by stepwise cooperative binding, *T. thermophilus* CarH only represses as an AdoCbl-bound tetramer using a DBD from one head-to-tail dimer to bind the −35 promoter element in the central repeat and the DBDs from the other dimer to bind the outer repeats (**Figure 5*c***) (38).

Structure of Light-Exposed CarH Suggests Mechanism of Photoregulation

The structure of light-exposed AdoCbl–CarH (**Figure 6*a***) clearly revealed bound Cbl without an Ado group and provided molecular insights into how light triggers tetramer disassembly (38). In the dark, the Ado group functions as a molecular doorstop by stacking against Trp131 [of the W-(9)x-EH motif] (**Figures 4*c*** and **6*b***). This interaction maintains the CarH protomer in the extended conformation required to assemble the head-to-tail dimer and thereby the tetramer. Once the Ado group dissociates upon exposure to light, Trp131 moves into the void caused by the loss of the Ado group, leading to a sizable shift (>8 Å) of the four-helix bundle relative to the Rossmann fold (**Figure 6*a***). The resulting bent conformation of the protomer disrupts the head-to-tail dimer interface, causing tetramer collapse and loss of DNA binding. The helix bundle shift repositions Trp131 and the adjacent His (His132), the latter of which ends up as the upper axial ligand of the Co in Cbl, forming a very stable bis–His ligation (**Figure 6*b*,*c***) (38). The structure of photolysed CarH provided the first visualization of a bis–His ligation involving Cbl. The very stable bis–His bond explains why fresh AdoCbl cannot replace Cbl in photolysed *T. thermophilus* CarH (38, 40). The biologically expensive Cbl is thus securely retained for recovery and reuse in vivo, although the details of the recovery process are not yet known. The lower axial His is the most strictly conserved residue of the canonical B_{12}-binding motif and is indispensable for cofactor binding and activity (37, 121, 129). By contrast, the upper axial His is not strictly required for tetramer assembly or its light-induced collapse. This His is conserved in thermophilic (38) and many other CarH homologs but not in all (e.g., it is a Glu in *M. xanthus* and *B. megaterium* CarH; **Figure 2*b***). A similar bis–His cobalt ligation was proposed in AerR, but the expected upper axial His is neither conserved nor is it in the putative four-helix bundle (130). Whether other residues can coordinate the Co on the upper site or another ligand such as water is involved remains to be explored.

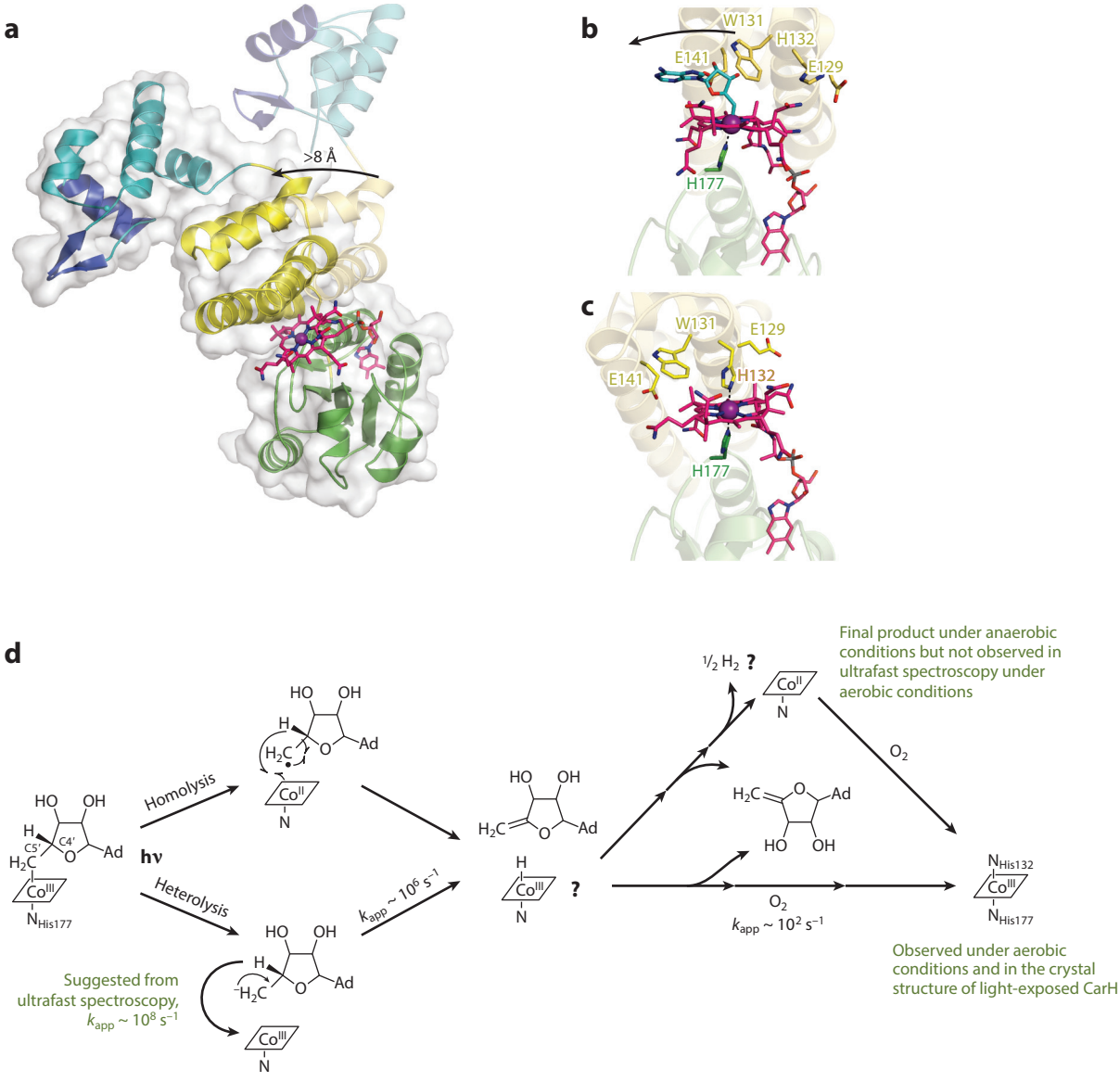

Figure 6

Molecular basis of photoregulation by CarH. (*a*) Structure of light-exposed CarH (*solid*, PDB accession code 5C8F) with the arrow indicating the major shift in the helix bundle relative to the dark structure (*transparent*, PDB accession code 5C8D). (*b*) Close-up of the AdoCbl binding site highlighting the role of the upper axial Ado group (*cyan*) of AdoCbl as a molecular doorstop in the dark state. The arrow indicates the helix bundle shift that occurs on exposure to light, leading to relocation of W131 and the other indicated residues. The nonconserved E129 was suggested to be involved in forming the bis–His adduct by deprotonating His132 on the basis of homology modeling and molecular dynamics studies (40), but this may be unlikely given its positioning in the crystal structure. (*c*) Close-up of the bis–His Co coordination in light-exposed CarH. (*d*) Scheme of the proposed mechanism for CarH photolysis adapted from Reference 39, with additional details from the high-resolution structures (38) and apparent rates (k_{app}) from transient kinetics data (40). The chemical structure of 4′,5′-anhydroadenosine, the product of AdoCbl photolysis in CarH (39), is shown in the middle (and to the right) of the scheme. Abbreviations: AdoCbl, 5′-deoxyadenosylcobalamin; CarH, B_{12}-dependent repressor of carotenogenesis; PDB, Protein Data Bank.

Photochemical Basis of CarH Function

The use of AdoCbl as a light sensor posed additional interesting questions regarding the photochemistry involved in the process. In particular, it seemed highly counterintuitive that a cell response to mitigate photooxidative damage by highly reactive ROS would rely on AdoCbl photolysis, as this process usually generates Ado•, which can itself produce ROS and trigger radical-induced cell damage. This apparent paradox prompted studies aimed at characterizing the products of CarH photolysis and the underlying photochemistry. In one study, the products of AdoCbl–CarH photolysis formed under aerobic or anaerobic conditions were analyzed using liquid chromatography–mass spectrometry and UV-visible, EPR, and NMR spectroscopies after sample workup on the timescale of minutes to hours (39). The other study involved transient kinetics analysis over femtoseconds to seconds using ultrafast spectroscopy, in which photolysis triggered by laser pulse excitation was followed by time-resolved acquisition of absorption spectra (40). These studies indicated that CarH orchestrates a distinct photochemistry to safeguard the use of AdoCbl as a light sensor and set the stage for further studies to elucidate the details.

Photolysis of free AdoCbl generates Ado•, which then forms a set of well-characterized products described earlier (5′-peroxyadenosine, adenosine-5′-aldehyde, and minor amounts of adenosine and adenine in the presence of oxygen, and 5′-deoxy-5′,8-cycloadenosine in the absence of oxygen) (71, 72). However, photolysis of CarH-bound AdoCbl did not yield any of these products but instead generated 4′,5′-anhydroadenosine (**Figure 6*d***), which had not been previously detected as a photolysis product of AdoCbl (39). 4′,5′-Anhydroadenosine had been observed as an inactivation product of some AdoCbl-dependent enzymes, the relevance and mechanism of which remain unclear (137, 138). More importantly, it was known to be a minor product of AdoCbl thermolysis via β-H elimination from the ribose C4′ of Ado•, primarily in viscous solvents when radical escape is slowed by solvent cage effects (139). The observation of 4′,5′-anhydroadenosine as the sole photolysis product thus directly suggested that CarH alters the photochemistry of AdoCbl and that the reactive Ado• is not released free into solution. In principle, two mechanistic routes could lead to formation of 4′,5′-anhydroadenosine (**Figure 6*d***). Photolysis could occur by Co–C bond homolysis to form cob(II) and Ado•, followed by β-H transfer from Ado• to cob(II) to form 4′,5′-anhydroadenosine and cob(III) hydride (hydridocobalamin), or it could occur by Co–C bond heterolysis to form cob(III) and an Ado^- anion, which could undergo β-hydride elimination to again yield 4′,5′-anhydroadenosine and cob(III) hydride (39). Under aerobic conditions, cob(III) hydride would become oxidized to the final bis–His-ligated cob(III) species observed in the crystal structure. Thus, either pathway yields the same end products, requiring characterization of the intermediates to distinguish between the pathways.

Analysis of the photochemical mechanism (over femtoseconds to seconds) of CarH-bound AdoCbl using ultrafast spectroscopy led to the conclusion that Co–C bond photolysis occurs primarily by a heterolytic mechanism (**Figure 6*d***), providing further evidence that CarH alters the photochemistry of AdoCbl (40). Although a small amount of homolytic cleavage was also observed, the resulting cob(II):Ado• radical pair underwent quantitative recombination. Thus, this study suggested that the photochemistry of CarH-bound AdoCbl is altered in two ways: Formation of Ado• is suppressed by activation of a heterolytic Co–C bond cleavage pathway, and any Ado• formed through homolytic Co–C bond cleavage is not released into solution (40).

The mechanistic basis for this altered photochemistry is still largely unclear. The UV-visible spectrum of CarH-bound AdoCbl, compared with free AdoCbl, exhibits some changes in the α and β absorption bands, including a shift of the α band to higher energy (38–40). Although these changes could point to a specific effect of the binding environment on the photochemistry, more studies are needed. In addition, CarH might exert a cage effect following photolytic cleavage of the

AdoCbl Co–C bond to suppress dissociation of Ado$^{\bullet}$ and Ado^{-} and instead favor β-H elimination. Similar cage effects have been observed in MetH and in the AdoCbl-dependent enzyme glutamate mutase, although in both cases these cage effects favor radical pair recombination and not a β-H elimination (104, 140, 141). Additionally, the observation that cob(II) is formed upon anaerobic photolysis of CarH seems at odds with heterolytic Co–C bond cleavage, although formation of cob(II) could be explained as a downstream consequence of cob(III) hydride decay (39). The contributions of specific amino acids are similarly unclear. The lack of conservation of His132, whose side chain occupies the B_{12} upper face following photolysis, suggests that its role may be specific to formation of bis–His-ligated cob(III). Instead, the conserved Trp, Glu, and His of the W-(9)x-EH motif, which interact with the Ado group in the dark-state CarH tetramer and orient the Ado group differently than is usually observed in enzyme-bound or free AdoCbl (**Figure 4*d***), could be involved in reprogramming AdoCbl photochemistry (37–40, 142), but again more work is needed. Detailed mechanistic studies using experimental as well as quantum mechanics/molecular mechanics approaches will help further elucidate the novel and promisingly rich photochemistry of CarH.

DISTRIBUTION AND EVOLUTIONARY ASPECTS OF B_{12}-DEPENDENT PHOTORECEPTORS

Genome searches yield hundreds of proteins with a MerR-type DBD fused to a B_{12}-binding domain in bacteria, only some of which are capable of de novo B_{12} biosynthesis. We could identify ∼600 proteins with the characteristic motifs found in experimentally studied CarH proteins and hence likely to be AdoCbl- and light-dependent: RxWxxR in the DBD and W-(9)x-EH [or W-(10)x-EH in many actinobacterial homologs, notably of the genus *Streptomyces*] preceding the E/DxH motif in the B_{12}-binding domain (**Figure 7**). Various other surrounding residues in the DBD and the B_{12}-binding domain are also conserved (**Figure 7*b***), hinting at their structural and functional importance. However, the His observed as the upper axial ligand in the bis–His cobalt of light-exposed *T. thermophilus* CarH (His132) is conserved only in some phyla, like Deinococcus-Thermus, suggesting a restricted functional role. One noteworthy feature is that the His of the W-(9)x-EH motif (His142 in *T. thermophilus*) and the Glu/Asp of the E/DxH of the B_{12}-binding motif (Glu175 in *T. thermophilus*) are typically spaced 32–39 residues apart (33–36 being most

Figure 7

Phylogenetic distribution of CarH and its B_{12}-binding domain in other proteins. (*a*) Distribution of the indicated domain architectures across different bacterial phyla, with the number of genomes for each phylum indicated (from ∼8,400 bacterial genomes, available at **http://www.ncbi.nlm.nih.gov/genomes**; for simplicity, only *Candidatus* phyla with relevant B_{12}-binding domains are shown). The number of proteins in each phylum (H, CarH; A, CarA) correspond to the color heat map (*bottom right*). InterPro (protein sequence analysis and classification, **https://www.ebi.ac.uk/interpro/**) was used to search for proteins with a B_{12}-binding domain (IPR006158) alone or in combination with a MerR-type DNA-binding domain (IPR000551) or other domains (IPR007024, globin-like; IPR005467, histidine kinase; IPR029016, GAF). Protein sequences retrieved from UniProt (Universal Protein Resource, **http://www.uniprot.org/**) were aligned using MUSCLE in MEGA7 (Molecular Evolutionary Genetics Analysis, **http://www.megasoftware.net/**). Those with the E/DxH B_{12}-binding motif preceded by a W-(9/10)x-EH motif were selected by manual curation. The ones fused to a MerR-type DBD with the RxWxxR motif were classified as CarH or, if they lacked the Trp but not the EH of the W-(9/10)x-EH motif, they were classified as CarA. The 200–260 residue size range was used to select for stand-alone proteins. (*b*) Sequence logo created using WebLogo (**http://weblogo.berkeley.edu/**) for 498 CarH proteins with the W-(9)x-EH motif [those with a W-(10)x-EH motif, mostly in Actinobacteria, were omitted]. Segments around signature residues (*asterisks*) used for curation in the DBD (*top left*, *cyan border*), the four-helix bundle (*top right*, *gold border*), and the Rossmann fold (*bottom*, *green border*) are shown. In the sequences (x, any residue) below each logo, conserved residues (≥95%) are highlighted in bold and larger font. Abbreviations: CarA, B_{12}-independent repressor of carotenogenesis; CarH, B_{12}-dependent repressor of carotenogenesis; DBD, DNA-binding domain; GAF, cGMP-specific phosphodiesterases, adenylyl cyclase, FhlA; MerR, mercury-sensing regulator.

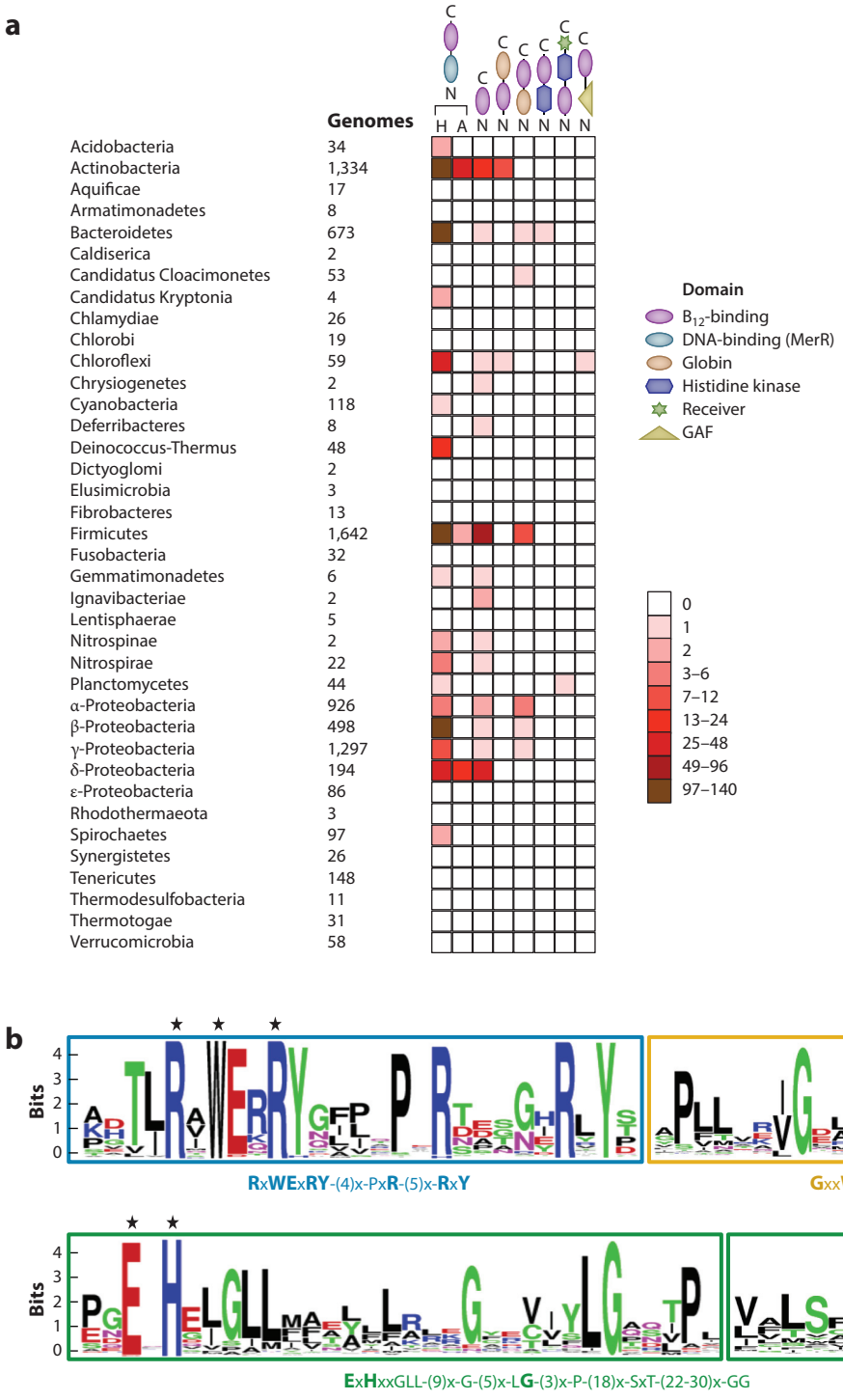
a
Genomes
H A N N N N N N
Acidobacteria 34
Actinobacteria 1,334
Aquificae 17
Armatimonadetes 8
Bacteroidetes 673
Caldiserica 2
Candidatus Cloacimonetes 53
Candidatus Kryptonia 4
Chlamydiae 26
Chlorobi 19
Chloroflexi 59
Chrysiogenetes 2
Cyanobacteria 118
Deferribacteres 8
Deinococcus-Thermus 48
Dictyoglomi 2
Elusimicrobia 3
Fibrobacteres 13
Firmicutes 1,642
Fusobacteria 32
Gemmatimonadetes 6
Ignavibacteriae 2
Lentisphaerae 5
Nitrospinae 2
Nitrospirae 22
Planctomycetes 44
α-Proteobacteria 926
β-Proteobacteria 498
γ-Proteobacteria 1,297
δ-Proteobacteria 194
ε-Proteobacteria 86
Rhodothermaeota 3
Spirochaetes 97
Synergistetes 26
Tenericutes 148
Thermodesulfobacteria 11
Thermotogae 31
Verrucomicrobia 58
Domain
B12-binding
DNA-binding (MerR)
Globin
Histidine kinase
Receiver
GAF
0
1
2
3–6
7–12
13–24
25–48
49–96
97–140
b
Bits
RxWExRY-(4)x-PxR-(5)x-RxY
GxxW-(9)x-EH-(32-39)x
ExHxxGLL-(9)x-G-(5)x-LG-(3)x-P-(18)x-SxT-(22-30)x-GG

common). Another is the rather wide distribution of linker size (~6–120 residues) between the DBD and the B_{12}-binding domain, which possibly underlies, as noted before, a rather flexible DNA binding mode. Altogether, the motifs shown in **Figure 7*b*** may serve as a signature for an AdoCbl-binding light-sensor module. The various putative CarH proteins are distributed across many bacterial phyla, being most abundant in Actinobacteria, Bacteroidetes, Chloroflexi, Deinococcus-Thermus, Firmicutes, and β- and δ-Proteobacteria (**Figure 7*a***). In most species, the corresponding genes are present as a single copy that, consistent with a light-response function, frequently occurs in the vicinity of genes for carotenogenesis or DNA photolyase. However, as observed in *B. megaterium* (129), *carH* can be involved in light-dependent regulation even when spatially decoupled in the genome from its target genes.

Proteins with CarH domain architecture but without the Trp of the W-(9)x-EH motif (and hence probably B_{12}-independent), like CarA, are less abundant (~60) and more narrowly distributed (Actinobacteria, Firmicutes, and δ-Proteobacteria) (**Figure 7*a***). The predominance of CarH proteins and their wider distribution suggests an ancestral protein that was more like CarH, a hypothesis in line with the distribution of CarH and CarA in the Myxococcales order of δ-Proteobacteria (25 and 10 proteins, respectively). Members of its Sorangiineae and Nannocystineae suborders have just one *carH* gene. *M. xanthus* and related species in the Cystobacterineae, however, have two tandem paralogous genes (*carA* and *carH*), as well as CarS and the full repertoire of other factors required in the B_{12}-independent CarA/CarS pathway, with *Cystobacter fuscus* standing out as the only one lacking CarA (M.C. Polanco, J. Fernández-Zapata, S. Padmanabhan & M. Elías-Arnanz, unpublished data). Taken together with the ancient origin proposed for B_{12} (48), the most parsimonious hypothesis is that the gene for an ancestral AdoCbl-dependent CarH duplicated and functionally diverged in Cystobacterineae to evolve into *carA*. Presence of *carH*, alone or in tandem with *carA*, in the neighborhood of genes for carotenogenesis in myxobacteria, suggests a common AdoCbl-dependent mode of regulation of this light-induced process, the alternative B_{12}-independent pathway coexisting in species with CarA. Having both pathways likely confers an evolutionary advantage, because the photoprotective carotenogenic response is maintained even in the absence of available B_{12}. It mirrors the coexistence of B_{12}-dependent and independent isozymes in many organisms that ensures crucial enzyme activities on limited B_{12} availability (48).

Besides B_{12}-dependent enzymes and CarH/CarA, genome data reveal the B_{12}-binding domain in a large number of proteins, stand-alone or linked to other effector/output domains (37, 143). In particular, a CarH-type AdoCbl-binding module with the characteristic W-(9)x-EH motif [again, W-(10)x-EH in *Streptomyces*] can be found in ~170 widely distributed stand-alone proteins (200–260 residues) (**Figure 7*a***). Notably, B_{12}-binding AerR/PpaA antirepressors, which are chromosomally coupled to CrtJ/PpsR and restricted to purple nonsulfur bacteria, appear to be distinct from CarH, lacking the characteristic motif (130, 131). In some cases, a CarH-type AdoCbl-binding module is associated with domains typically involved in signal transduction (**Figure 7*a***), such as globin (heme-based oxygen sensor), histidine kinase, or GAF (cGMP-specific phosphodiesterases, adenylyl cyclase, FhlA) (144). Their functions and modes of action remain uncharted, but it is tempting to speculate that these exhibit AdoCbl- and light-dependent protein–protein interactions with themselves (like CarH) and/or with other effector proteins. The stage has thus been set for future studies of the function and evolution of these putative B_{12}-binding proteins.

CONCLUDING REMARKS AND OUTLOOK

The discovery that AdoCbl is the chromophore of a new family of photoreceptors changed the perception that a basic property of AdoCbl, its light sensitivity, has no direct biological function.

Major landmarks have been reached in understanding the mechanism of action of the first known photoreceptor of this class, CarH, including characterization of its distinct photochemistry and high-resolution structural descriptions of its functionally relevant states. These studies have illustrated how nature has assembled a light- and B_{12}-dependent transcription factor by repurposing structural modules of enzymes and DNA-binding proteins and repurposing AdoCbl from an enzyme cofactor into a light sensor. Genome data reveal similar B_{12}-binding domains in a plethora of organisms; these domains are stand-alone or linked to other modules that could allow for integration of signals and regulation of diverse biological processes. Their study will surely be a rich source for the identification of new modes of B_{12}- and light-dependent regulation and possible cross-talk between distinct signaling pathways. Future surprises are certainly in store, given the precedent set by studies thus far. Undoubtedly, innovative experimental and theoretical approaches will address the various remaining questions on the molecular mechanisms of B_{12}-based photoreception. Whereas light induces reversible molecular changes in the chromophore of other photoreceptors (31, 32), it alters the chromophore irreversibly for the AdoCbl-dependent photoreceptor. The latter suggests that specialized cellular salvage and repair pathways may exist that remain to be discovered. Another exciting research avenue concerns possible applications of these photoreceptors. In initial studies, CarH has been exploited for light- and B_{12}-dependent conditional expression of essential bacterial genes (145). In a promising new development, it has been used as an optogenetic tool to regulate, using green light, receptor interactions and signaling in human cells as well as during development in zebra fish embryos (146). Whether it can be optimized for additional optogenetic applications remains to be seen. In any case, the study of these photoreceptors has already uncovered fascinating new biology and chemistry and promises many more surprises in the future.

SUMMARY POINTS

1. A new family of photoreceptors uses AdoCbl or coenzyme B_{12} as a chromophore to sense near-UV, blue, and green light.
2. The first characterized AdoCbl-dependent photoreceptor, the CarH transcription factor, is a tetramer that represses transcription of genes involved in carotenoid biosynthesis in the dark. Light causes the CarH-bound AdoCbl to photolyse, leading to a large protein conformational change that disrupts the tetramer, impairing DNA binding and abolishing transcription repression.
3. The photochemistry of the AdoCbl-based photoreceptor appears to be distinct from that of free and enzyme-bound AdoCbl. The altered photochemistry provides a means to safeguard the use of AdoCbl as a light sensor. The underlying molecular basis for the difference in photochemistry remains an open question.
4. In another mode of light- and B_{12}-dependent gene regulation, light induces cobalamin binding to an antirepressor, which then binds to its target repressor to activate transcription.
5. Genome data reveal B_{12}-binding modules similar to the one in CarH associated with various other domains or existing as stand-alone proteins, the functions of which are unknown.

FUTURE ISSUES

1. The structural basis for the variations in the oligomerization behavior of AdoCbl-dependent photoreceptors is not known. For example, why some tetramers disassemble to dimers whereas others disassemble to monomers is unclear.
2. More evidence is needed to support the proposal that the variation in linker length between the CarH DNA-binding domains and light-sensing domains explains the apparently flexible modes of DNA binding of CarH homologs.
3. The exact role(s) of the protein residues around the Ado group in CarH remain to be determined. Which residues, if any, are responsible for the distinct photochemistry of CarH is unclear.
4. Theoretical (quantum mechanics, molecular mechanics) approaches will be helpful in understanding the photochemistry of AdoCbl-bound CarH.
5. The intracellular fates of the photolysed photoreceptor and its associated chromophore remain to be established, as do the cellular machineries involved in determining these fates.
6. Whether other physiological processes are regulated by AdoCbl-based light sensing is an open question.
7. The use of B_{12}-based photoreceptors as an optogenetic tool, which appears promising, requires further study.

DISCLOSURE STATEMENT

The authors are not aware of any affiliations, memberships, funding, or financial holdings that might be perceived as affecting the objectivity of this review.

ACKNOWLEDGMENTS

We apologize for any relevant work not cited owing to space constraints. This work was supported by grants from the Ministerio de Economía and Competitividad of Spain [BFU2015–67968-C2–1-P, cofinanced by FEDER (Fondo Europeo de Desarrollo Regional), to M.E.-A.; BFU2015–67968-C22-P to S.P.] and Fundación Séneca of Spain (19429/PI/14 to M.E.-A). C.L.D. is a Howard Hughes Medical Institute Investigator with support from the National Institutes of Health (GM69857). M.J. was funded by National Institutes of Health grant F32 GM116331.

LITERATURE CITED

1. Croce R, van Amerongen H. 2014. Natural strategies for photosynthetic light harvesting. *Nat. Chem. Biol.* 10:492–501
2. Palczewski K. 2012. Chemistry and biology of vision. *J. Biol. Chem.* 287:1612–19
3. Wald G. 1968. The molecular basis of visual excitation. *Nature* 219:800–7
4. Cohen SE, Golden SS. 2015. Circadian rhythms in cyanobacteria. *Microbiol. Mol. Biol. Rev.* 79:373–85
5. Nagel DH, Kay SA. 2012. Complexity in the wiring and regulation of plant circadian networks. *Curr. Biol.* 22:R648–57

6. Chaves I, Pokorny R, Byrdin M, Hoang N, Ritz T, et al. 2011. The cryptochromes: blue light photoreceptors in plants and animals. *Annu. Rev. Plant Biol.* 62:335–64
7. Sancar A, Lindsey-Boltz LA, Kang TH, Reardon JT, Lee JH, Ozturk N. 2010. Circadian clock control of the cellular response to DNA damage. *FEBS Lett.* 584:2618–25
8. Fankhauser C, Christie JM. 2015. Plant phototropic growth. *Curr. Biol.* 25:R384–89
9. Ballaré CL. 2014. Light regulation of plant defense. *Annu. Rev. Plant Biol.* 65:335–63
10. Swartz TE, Tseng TS, Frederickson MA, Paris G, Comerci DJ, et al. 2007. Blue-light-activated histidine kinases: two-component sensors in bacteria. *Science* 317:1090–93
11. Elías-Arnanz M, Padmanabhan S, Murillo FJ. 2011. Light-dependent gene regulation in nonphototrophic bacteria. *Curr. Opin. Microbiol.* 14:128–35
12. Purcell EB, Crosson S. 2008. Photoregulation in prokaryotes. *Curr. Opin. Microbiol.* 11:168–78
13. Crane BR, Young MW. 2014. Interactive features of proteins composing eukaryotic circadian clocks. *Annu. Rev. Biochem.* 83:191–219
14. Ziegelhoffer EC, Donohue TJ. 2009. Bacterial responses to photo-oxidative stress. *Nat. Rev. Microbiol.* 7:856–63
15. Li Z, Wakao S, Fischer BB, Niyogi KK. 2009. Sensing and responding to excess light. *Annu. Rev. Plant Biol.* 60:239–60
16. Glaeser J, Nuss AM, Berghoff BA, Klug G. 2011. Singlet oxygen stress in microorganisms. *Adv. Microb. Physiol.* 58:141–73
17. Latifi A, Ruiz M, Zhang CC. 2009. Oxidative stress in cyanobacteria. *FEMS Microbiol. Rev.* 33:258–78
18. Setlow RB. 1966. Cyclobutane-type pyrimidine dimers in polynucleotides. *Science* 153:379–86
19. Erickson E, Wakao S, Niyogi KK. 2015. Light stress and photoprotection in *Chlamydomonas reinhardtii*. *Plant J.* 82:449–65
20. Christie JM, Arvai AS, Baxter KJ, Heilmann M, Pratt AJ, et al. 2012. Plant UVR8 photoreceptor senses UV-B by tryptophan-mediated disruption of cross-dimer salt bridges. *Science* 335:1492–96
21. Wu D, Hu Q, Yan Z, Chen W, Yan C, et al. 2012. Structural basis of ultraviolet-B perception by UVR8. *Nature* 484:214–19
22. Genick UK, Soltis SM, Kuhn P, Canestrelli IL, Getzoff ED. 1998. Structure at 0.85 Å resolution of an early protein photocycle intermediate. *Nature* 392:206–9
23. Herrou J, Crosson S. 2011. Function, structure and mechanism of bacterial photosensory LOV proteins. *Nat. Rev. Microbiol.* 9:713–23
24. Leverenz RL, Sutter M, Wilson A, Gupta S, Thurotte A, et al. 2015. A 12 Å carotenoid translocation in a photoswitch associated with cyanobacterial photoprotection. *Science* 348:1463–66
25. Losi A, Gärtner W. 2012. The evolution of flavin-binding photoreceptors: an ancient chromophore serving trendy blue-light sensors. *Annu. Rev. Plant Biol.* 63:49–72
26. Masuda S. 2013. Light detection and signal transduction in the BLUF photoreceptors. *Plant Cell Physiol.* 54:171–79
27. Sancar A. 2003. Structure and function of DNA photolyase and cryptochrome blue-light photoreceptors. *Chem. Rev.* 103:2203–37
28. Wilson A, Punginelli C, Gall A, Bonetti C, Alexandre M, et al. 2008. A photoactive carotenoid protein acting as light intensity sensor. *PNAS* 105:12075–80
29. Anders K, Essen LO. 2015. The family of phytochrome-like photoreceptors: diverse, complex and multicolored, but very useful. *Curr. Opin. Struct. Biol.* 35:7–16
30. Rockwell NC, Su Y-S, Lagarias JC. 2006. Phytochrome structure and signaling mechanisms. *Annu. Rev. Plant Biol.* 57:837–58
31. Möglich A, Yang X, Ayers RA, Moffat K. 2010. Structure and function of plant photoreceptors. *Annu. Rev. Plant Biol.* 61:21–47
32. Shcherbakova DM, Shemetov AA, Kaberniuk AA, Verkhusha VV. 2015. Natural photoreceptors as a source of fluorescent proteins, biosensors, and optogenetic tools. *Annu. Rev. Biochem.* 84:519–50
33. Bhattacharyya RP, Reményi A, Yeh BJ, Lim WA. 2006. Domains, motifs, and scaffolds: the role of modular interactions in the evolution and wiring of cell signaling circuits. *Annu. Rev. Biochem.* 75:655–80
34. Fenno L, Yizhar O, Deisseroth K. 2011. The development and application of optogenetics. *Annu. Rev. Neurosci.* 34:389–412

35. Miesenböck G. 2011. Optogenetic control of cells and circuits. *Annu. Rev. Cell Dev. Biol.* 27:731–58
36. Zhang K, Cui B. 2015. Optogenetic control of intracellular signaling pathways. *Trends Biotechnol.* 33:92–100
37. Ortiz-Guerrero JM, Polanco MC, Murillo FJ, Padmanabhan S, Elías-Arnanz M. 2011. Light-dependent gene regulation by a coenzyme B_{12}-based photoreceptor. *PNAS* 108:7565–70
38. Jost M, Fernández-Zapata J, Polanco MC, Ortiz-Guerrero JM, Chen PY, et al. 2015. Structural basis for gene regulation by a B_{12}-dependent photoreceptor. *Nature* 526:536–41
39. Jost M, Simpson JH, Drennan CL. 2015. The transcription factor CarH safeguards use of adenosylcobalamin as a light sensor by altering the photolysis products. *Biochemistry* 54:3231–34
40. Kutta RJ, Hardman SJ, Johannissen LO, Bellina B, Messiha HL, et al. 2015. The photochemical mechanism of a B_{12}-dependent photoreceptor protein. *Nat. Commun.* 6:7907
41. Whipple GH, Robscheit-Robbins FS. 1925. Favourable influence of liver, heart and skeletal muscle in diet on blood regeneration in anemia. *Am. J. Physiol.* 72:408–18
42. Minot GR, Murphy WP. 1926. Treatment of pernicious anemia by a special diet. *J. Am. Med. Assoc.* 87:470–76
43. Rickes EL, Brink NG, Koniuszy FR, Wood TR, Folkers K. 1948. Crystalline vitamin B_{12}. *Science* 107:396–97
44. Smith EL. 1948. Purification of anti-pernicious anaemia factors from liver. *Nature* 161:638
45. Hodgkin DC, Kamper J, Mackay M, Pickworth J, Trueblood KN, White JG. 1956. Structure of vitamin B_{12}. *Nature* 178:64–66
46. Eschenmoser A, Wintner CE. 1977. Natural product synthesis and vitamin B_{12}. *Science* 196:1410–20
47. Croft MT, Lawrence AD, Raux-Deery E, Warren MJ, Smith AG. 2005. Algae acquire vitamin B_{12} through a symbiotic relationship with bacteria. *Nature* 438:90–93
48. Roth JR, Lawrence JG, Bobik TA. 1996. Cobalamin (coenzyme B_{12}): synthesis and biological significance. *Annu. Rev. Microbiol.* 50:137–81
49. Taga ME, Larsen NA, Howard-Jones AR, Walsh CT, Walker GC. 2007. BluB cannibalizes flavin to form the lower ligand of vitamin B_{12}. *Nature* 446:449–53
50. Warren MJ, Raux E, Schubert HL, Escalante-Semerena JC. 2002. The biosynthesis of adenosylcobalamin (vitamin B_{12}). *Nat. Prod. Rep.* 19:390–412
51. Rodionov DA, Vitreschak AG, Mironov AA, Gelfand MS. 2003. Comparative genomics of the vitamin B_{12} metabolism and regulation in prokaryotes. *J. Biol. Chem.* 278:41148–59
52. Zhang Y, Rodionov DA, Gelfand MS, Gladyshev VN. 2009. Comparative genomic analyses of nickel, cobalt and vitamin B_{12} utilization. *BMC Genom.* 10:78
53. Degnan PH, Taga ME, Goodman AL. 2014. Vitamin B_{12} as a modulator of gut microbial ecology. *Cell Metab.* 20:769–78
54. Banerjee R, Ragsdale SW. 2003. The many faces of vitamin B_{12}: catalysis by cobalamin-dependent enzymes. *Annu. Rev. Biochem.* 72:209–47
55. Ludwig ML, Matthews RG. 1997. Structure-based perspectives on B_{12}-dependent enzymes. *Annu. Rev. Biochem.* 66:269–313
56. Lenhert PG, Hodgkin DC. 1961. Structure of the 5,6-dimethyl-benzimidazolylcobamide coenzyme. *Nature* 192:937–38
57. Rossi R, Glusker JP, Randaccio L, Summers MF, Toscano PJ, Marzilli LG. 1985. The structure of a B_{12} coenzyme: methylcobalamin studies by X-ray and NMR methods. *J. Am. Chem. Soc.* 107:1729–38
58. Hung RR, Grabowski JJ. 1999. Listening to reactive intermediates: application of photoacoustic calorimetry to vitamin B_{12} compounds. *J. Am. Chem. Soc.* 121:1351–64
59. Hay BP, Finke RG. 1986. Thermolysis of the cobalt-carbon bond of adenosylcobalamin. 2. Products, kinetics, and cobalt-carbon bond dissociation energy in aqueous solution. *J. Am. Chem. Soc.* 108:4820–29
60. Randaccio L, Geremia S, Demitri N, Wuerges J. 2010. Vitamin B_{12}: unique metalorganic compounds and the most complex vitamins. *Molecules* 15:3228–59
61. Kozlowski PM, Garabato BD, Lodowski P, Jaworska M. 2016. Photolytic properties of cobalamins: a theoretical perspective. *Dalton Trans.* 45:4457–70
62. Rury AS, Wiley TE, Sension RJ. 2015. Energy cascades, excited state dynamics, and photochemistry in cob(III)alamins and ferric porphyrins. *Acc. Chem. Res.* 48:860–67

63. Gruber K, Puffer B, Kräutler B. 2011. Vitamin B_{12}-derivatives—enzyme cofactors and ligands of proteins and nucleic acids. *Chem. Soc. Rev.* 40:4346–63
64. Drennan CL, Huang S, Drummond JT, Matthews RG, Ludwig ML. 1994. How a protein binds B_{12}: a 3.0 Å X-ray structure of B_{12}-binding domains of methionine synthase. *Science* 266:1669–74
65. Liptak MD, Brunold TC. 2006. Spectroscopic and computational studies of Co^{1+}cobalamin: spectral and electronic properties of the "superreduced" B_{12} cofactor. *J. Am. Chem. Soc.* 128:9144–56
66. Stich TA, Brooks AJ, Buan NR, Brunold TC. 2003. Spectroscopic and computational studies of Co^{3+}-corrinoids: spectral and electronic properties of the B_{12} cofactors and biologically relevant precursors. *J. Am. Chem. Soc.* 125:5897–914
67. Stich TA, Buan NR, Brunold TC. 2004. Spectroscopic and computational studies of Co^{2+}corrinoids: spectral and electronic properties of the biologically relevant base-on and base-off forms of Co^{2+}cobalamin. *J. Am. Chem. Soc.* 126:9735–49
68. Shell TA, Lawrence DS. 2011. A new trick (hydroxyl radical generation) for an old vitamin (B_{12}). *J. Am. Chem. Soc.* 133:2148–50
69. Wiley TE, Miller WR, Miller NA, Sension RJ, Lodowski P, et al. 2016. Photostability of hydroxocobalamin: ultrafast excited state dynamics and computational studies. *J. Phys. Chem. Lett.* 7:143–47
70. Schwartz PA, Frey PA. 2007. 5′-Peroxyadenosine and 5′-peroxyadenosylcobalamin as intermediates in the aerobic photolysis of adenosylcobalamin. *Biochemistry* 46:7284–92
71. Hogenkamp HP. 1963. A cyclic nucleoside derived from coenzyme B_{12}. *J. Biol. Chem.* 238:477–80
72. Hogenkamp HP. 1966. The photolysis of methylcobalamin. *Biochemistry* 5:417–22
73. Law PY, Wood JM. 1973. The photolysis of 5′-deoxyadenosylcobalamin under anaerobic conditions. *Biochim. Biophys. Acta* 331:451–54
74. Chen E, Chance MR. 1990. Nanosecond transient absorption spectroscopy of coenzyme B_{12}. Quantum yields and spectral dynamics. *J. Biol. Chem.* 265:12987–94
75. Endicott JF, Netzel TL. 1979. Early events and transient chemistry in the photohomolysis of alkylcobalamins. *J. Am. Chem. Soc.* 101:4000–2
76. Jones AR, Russell HJ, Greetham GM, Towrie M, Hay S, Scrutton NS. 2012. Ultrafast infrared spectral fingerprints of vitamin B_{12} and related cobalamins. *J. Phys. Chem. A* 116:5586–94
77. Walker LA, Jarett JT, Anderson NA, Pullen SH, Matthews RG, Sension RJ. 1998. Time-resolved spectroscopic studies of B_{12} coenzymes: the identification of a metastable cob(III)alamin photoproduct in the photolysis of methylcobalamin. *J. Am. Chem. Soc.* 120:3597–603
78. Walker LA, Shiang JJ, Anderson NA, Pullen SH, Sension RJ. 1998. Time-resolved spectroscopic studies of B_{12} coenzymes: the photolysis and geminate recombination of adenosylcobalamin. *J. Am. Chem. Soc.* 120:7286–92
79. Stickrath AB, Carroll EC, Dai X, Harris DA, Rury A, et al. 2009. Solvent-dependent cage dynamics of small nonpolar radicals: lessons from the photodissociation and geminate recombination of alkylcobalamins. *J. Phys. Chem. A* 113:8513–22
80. Yamada R, Shimizu S, Fukui S. 1966. Factors affecting the anaerobic photolysis of the cobalt-carbon bond of cobalt-methylcobalamin. *Biochim. Biophys. Acta* 124:195–97
81. Deery E, Schroeder S, Lawrence AD, Taylor SL, Seyedarabi A, et al. 2012. An enzyme-trap approach allows isolation of intermediates in cobalamin biosynthesis. *Nat. Chem. Biol.* 8:933–40
82. Hazra AB, Han AW, Mehta AP, Mok KC, Osadchiy V, et al. 2015. Anaerobic biosynthesis of the lower ligand of vitamin B_{12}. *PNAS* 112:10792–97
83. Moore SJ, Lawrence AD, Biedendieck R, Deery E, Frank S, et al. 2013. Elucidation of the anaerobic pathway for the corrin component of cobalamin (vitamin B_{12}). *PNAS* 110:14906–11
84. Yin L, Bauer CE. 2013. Controlling the delicate balance of tetrapyrrole biosynthesis. *Philos. Trans. R. Soc. B* 368:20120262
85. Banerjee R, Gherasim C, Padovani D. 2009. The tinker, tailor, soldier in intracellular B_{12} trafficking. *Curr. Opin. Chem. Biol.* 13:484–91
86. Cracan V, Banerjee R. 2013. Cobalt and corrinoid transport and biochemistry. *Met. Ions Life Sci.* 12:333–74
87. Fedosov SN. 2012. Physiological and molecular aspects of cobalamin transport. *Subcell. Biochem.* 56:347–67

88. Nielsen MJ, Rasmussen MR, Andersen CB, Nexø E, Moestrup SK. 2012. Vitamin B_{12} transport from food to the body's cells—a sophisticated, multistep pathway. *Nat. Rev. Gastroenterol. Hepatol.* 9:345–54
89. Yamanishi M, Vlasie M, Banerjee R. 2005. Adenosyltransferase: an enzyme and an escort for coenzyme B_{12}? *Trends Biochem. Sci.* 30:304–8
90. Jost M, Cracan V, Hubbard PA, Banerjee R, Drennan CL. 2015. Visualization of a radical B_{12} enzyme with its G-protein chaperone. *PNAS* 112:2419–24
91. Gherasim C, Lofgren M, Banerjee R. 2013. Navigating the B_{12} road: assimilation, delivery, and disorders of cobalamin. *J. Biol. Chem.* 288:13186–93
92. Johnson CL, Pechonick E, Park SD, Havemann GD, Leal NA, Bobik TA. 2001. Functional genomic, biochemical, and genetic characterization of the *Salmonella pduO* gene, an ATP:cob(I)alamin adenosyltransferase gene. *J. Bacteriol.* 183:1577–84
93. Dowling DP, Croft AK, Drennan CL. 2012. Radical use of Rossmann and TIM barrel architectures for controlling coenzyme B_{12} chemistry. *Annu. Rev. Biophys.* 41:403–27
94. Giedyk M, Goliszewska K, Gryko D. 2015. Vitamin B_{12} catalysed reactions. *Chem. Soc. Rev.* 44:3391–404
95. Ludwig ML, Drennan CL, Matthews RG. 1996. The reactivity of B_{12} cofactors: The proteins make a difference. *Structure* 4:505–12
96. Jones AR, Levy C, Hay S, Scrutton NS. 2013. Relating localized protein motions to the reaction coordinate in coenzyme B_{12}-dependent enzymes. *FEBS J.* 280:2997–3008
97. Sukumar N. 2013. Crystallographic studies on B_{12} binding proteins in eukaryotes and prokaryotes. *Biochimie* 95:976–88
98. Bommer M, Kunze C, Fesseler J, Schubert T, Diekert G, Dobbek H. 2014. Structural basis for organohalide respiration. *Science* 346:455–58
99. Payne KA, Quezada CP, Fisher K, Dunstan MS, Collins FA, et al. 2015. Reductive dehalogenase structure suggests a mechanism for B_{12}-dependent dehalogenation. *Nature* 517:513–16
100. Dowling DP, Miles ZD, Kohrer C, Maiocco SJ, Elliott SJ, et al. 2016. Molecular basis of cobalamin-dependent RNA modification. *Nucleic Acids Res.* 44:9965–76
101. Payne KA, Fisher K, Sjuts H, Dunstan MS, Bellina B, et al. 2015. Epoxyqueuosine reductase structure suggests a mechanism for cobalamin-dependent tRNA modification. *J. Biol. Chem.* 290:27572–81
102. Goulding CW, Postigo D, Matthews RG. 1997. Cobalamin-dependent methionine synthase is a modular protein with distinct regions for binding homocysteine, methyltetrahydrofolate, cobalamin, and adenosylmethionine. *Biochemistry* 36:8082–91
103. Matthews RG, Koutmos M, Datta S. 2008. Cobalamin-dependent and cobamide-dependent methyltransferases. *Curr. Opin. Struct. Biol.* 18:658–66
104. Jarrett JT, Drennan CL, Amaratunga M, Scholten JD, Ludwig ML, Matthews RG. 1996. A protein radical cage slows photolysis of methylcobalamin in methionine synthase from *Escherichia coli*. *Bioorg. Med. Chem.* 4:1237–46
105. Mandal M, Breaker RR. 2004. Gene regulation by riboswitches. *Nat. Rev. Mol. Cell Biol.* 5:451–63
106. Serganov A, Patel DJ. 2012. Metabolite recognition principles and molecular mechanisms underlying riboswitch function. *Annu. Rev. Biophys.* 41:343–70
107. Nahvi A, Barrick JE, Breaker RR. 2004. Coenzyme B_{12} riboswitches are widespread genetic control elements in prokaryotes. *Nucleic Acids Res.* 32:143–50
108. Johnson JE Jr., Reyes FE, Polaski JT, Batey RT. 2012. B_{12} cofactors directly stabilize an mRNA regulatory switch. *Nature* 492:133–37
109. Peselis A, Serganov A. 2012. Structural insights into ligand binding and gene expression control by an adenosylcobalamin riboswitch. *Nat. Struct. Mol. Biol.* 19:1182–84
110. Elías-Arnanz M, Fontes M, Padmanabhan S. 2008. Carotenogenesis in *Myxococcus xanthus*: a complex regulatory network. In *Myxobacteria: Multicellularity and Differentiation*, ed. DE Whitworth, pp. 211–25. Washington, DC: ASM Press
111. Armstrong GA. 1997. Genetics of eubacterial carotenoid biosynthesis: a colorful tale. *Annu. Rev. Microbiol.* 51:629–59
112. Galbis-Martínez M, Padmanabhan S, Murillo FJ, Elías-Arnanz M. 2012. CarF mediates signaling by singlet oxygen, generated via photoexcited protoporphyrin IX, in *Myxococcus xanthus* light-induced carotenogenesis. *J. Bacteriol.* 194:1427–36

113. Cervantes M, Murillo FJ. 2002. Role for vitamin B_{12} in light induction of gene expression in the bacterium *Myxococcus xanthus*. *J. Bacteriol.* 184:2215–24
114. Chang CC, Lin LY, Zou XW, Huang CC, Chan NL. 2015. Structural basis of the mercury(II)-mediated conformational switching of the dual-function transcriptional regulator MerR. *Nucleic Acids Res.* 43:7612–23
115. Heldwein EE, Brennan RG. 2001. Crystal structure of the transcription activator BmrR bound to DNA and a drug. *Nature* 409:378–82
116. Philips SJ, Canalizo-Hernandez M, Yildirim I, Schatz GC, Mondragón A, O'Halloran TV. 2015. Allosteric transcriptional regulation via changes in the overall topology of the core promoter. *Science* 349:877–81
117. Martell DJ, Joshi CP, Gaballa A, Santiago AG, Chen TY, et al. 2015. Metalloregulator CueR biases RNA polymerase's kinetic sampling of dead-end or open complex to repress or activate transcription. *PNAS* 112:13467–72
118. Botella JA, Murillo FJ, Ruiz-Vázquez R. 1995. A cluster of structural and regulatory genes for light-induced carotenogenesis in *Myxococcus xanthus*. *Eur. J. Biochem.* 233:238–48
119. Navarro-Avilés G, Jiménez MA, Pérez-Marín MC, González C, Rico M, et al. 2007. Structural basis for operator and antirepressor recognition by *Myxococcus xanthus* CarA repressor. *Mol. Microbiol.* 63:980–94
120. Pérez-Marín MC, López-Rubio JJ, Murillo FJ, Elías-Arnanz M, Padmanabhan S. 2004. The N terminus of *Myxococcus xanthus* CarA repressor is an autonomously folding domain that mediates physical and functional interactions with both operator DNA and antirepressor protein. *J. Biol. Chem.* 279:33093–103
121. Pérez-Marín MC, Padmanabhan S, Polanco MC, Murillo FJ, Elías-Arnanz M. 2008. Vitamin B_{12} partners the CarH repressor to downregulate a photoinducible promoter in *Myxococcus xanthus*. *Mol. Microbiol.* 67:804–19
122. López-Rubio JJ, Elías-Arnanz M, Padmanabhan S, Murillo FJ. 2002. A repressor-antirepressor pair links two loci controlling light-induced carotenogenesis in *Myxococcus xanthus*. *J. Biol. Chem.* 277:7262–70
123. López-Rubio JJ, Padmanabhan S, Lázaro JM, Salas M, Murillo FJ, Elías-Arnanz M. 2004. Operator design and mechanism for CarA repressor-mediated down-regulation of the photoinducible *carB* operon in *Myxococcus xanthus*. *J. Biol. Chem.* 279:28945–53
124. Whitworth DE, Hodgson DA. 2001. Light-induced carotenogenesis in *Myxococcus xanthus*: evidence that CarS acts as an anti-repressor of CarA. *Mol. Microbiol.* 42:809–19
125. León E, Navarro-Avilés G, Santiveri CM, Flores-Flores C, Rico M, et al. 2010. A bacterial antirepressor with SH3 domain topology mimics operator DNA in sequestering the repressor DNA recognition helix. *Nucleic Acids Res.* 38:5226–41
126. Takano H, Obitsu S, Beppu T, Ueda K. 2005. Light-induced carotenogenesis in *Streptomyces coelicolor* A3(2): identification of an extracytoplasmic function sigma factor that directs photodependent transcription of the carotenoid biosynthesis gene cluster. *J. Bacteriol.* 187:1825–32
127. Díez AI, Ortiz-Guerrero JM, Ortega A, Elías-Arnanz M, Padmanabhan S, García de la Torre J. 2013. Analytical ultracentrifugation studies of oligomerization and DNA-binding of TtCarH, a *Thermus thermophilus* coenzyme B_{12}-based photosensory regulator. *Eur. Biophys. J.* 42:463–76
128. Takano H, Kondo M, Usui N, Usui T, Ohzeki H, et al. 2011. Involvement of CarA/LitR and CRP/FNR family transcriptional regulators in light-induced carotenoid production in *Thermus thermophilus*. *J. Bacteriol.* 193:2451–59
129. Takano H, Mise K, Hagiwara K, Hirata N, Watanabe S, et al. 2015. Role and function of LitR, an adenosyl B_{12}-bound light-sensitive regulator of *Bacillus megaterium* QM B1551, in regulation of carotenoid production. *J. Bacteriol.* 197:2301–15
130. Cheng Z, Li K, Hammad LA, Karty JA, Bauer CE. 2014. Vitamin B_{12} regulates photosystem gene expression via the CrtJ antirepressor AerR in *Rhodobacter capsulatus*. *Mol. Microbiol.* 91:649–64
131. Vermeulen AJ, Bauer CE. 2015. Members of the PpaA/AerR antirepressor family bind cobalamin. *J. Bacteriol.* 197:2694–703
132. Ponnampalam SN, Bauer CE. 1997. DNA binding characteristics of CrtJ. A redox-responding repressor of bacteriochlorophyll, carotenoid, and light harvesting-II gene expression in *Rhodobacter capsulatus*. *J. Biol. Chem.* 272:18391–96

133. Ponnampalam SN, Buggy JJ, Bauer CE. 1995. Characterization of an aerobic repressor that coordinately regulates bacteriochlorophyll, carotenoid, and light harvesting-II expression in *Rhodobacter capsulatus*. *J. Bacteriol.* 177:2990–97
134. Edayathumangalam R, Wu R, Garcia R, Wang Y, Wang W, et al. 2013. Crystal structure of *Bacillus subtilis* GabR, an autorepressor and transcriptional activator of *gabT*. *PNAS* 110:17820–25
135. Al-Zyoud WA, Hynson RM, Ganuelas LA, Coster AC, Duff AP, et al. 2016. Binding of transcription factor GabR to DNA requires recognition of DNA shape at a location distinct from its cognate binding site. *Nucleic Acids Res.* 44:1411–20
136. Ohlendorf R, Schumacher CH, Richter F, Möglich A. 2016. Library-aided probing of linker determinants in hybrid photoreceptors. *ACS Synth. Biol.* 5:1117–26
137. Katz RN, Vickrey TM, Schrauzer GN. 1976. Detection of 4′,5′-anhydroadenosine as the cleavage product of coenzyme B_{12} in functional holoenzymes. *Angew. Chem. Int. Ed. Engl.* 15:542–43
138. Krouwer JS, Schultz RM, Babior BM. 1978. The mechanism of action of ethanolamine ammonia-lyase, an adenosylcobalamin-dependent enzyme. Reaction of the enzyme cofactor complex with 2-aminoacetaldehyde. *J. Biol. Chem.* 253:1041–47
139. Garr CD, Finke RG. 1993. Adocobalamin (AdoCbl or coenzyme B_{12}) cobalt-carbon bond homolysis radical-cage effects: product, kinetic, mechanistic, and cage efficiency factor (F_c) studies, plus the possibility that coenzyme B_{12}-dependent enzymes function as "ultimate radical cages" and "ultimate radical traps." *Inorg. Chem.* 32:4414–21
140. Sension RJ, Cole AG, Harris AD, Fox CC, Woodbury NW, et al. 2004. Photolysis and recombination of adenosylcobalamin bound to glutamate mutase. *J. Am. Chem. Soc.* 126:1598–99
141. Sension RJ, Harris DA, Stickrath A, Cole AG, Fox CC, Marsh EN. 2005. Time-resolved measurements of the photolysis and recombination of adenosylcobalamin bound to glutamate mutase. *J. Phys. Chem. B* 109:18146–52
142. Gruber K, Kräutler B. 2016. Coenzyme B_{12} repurposed for photoregulation of gene expression. *Angew. Chem. Int. Ed. Engl.* 55:5638–40
143. Cheng Z, Yamamoto H, Bauer CE. 2016. Cobalamin's (vitamin B_{12}) surprising function as a photoreceptor. *Trends Biochem. Sci.* 41:647–50
144. Martinkova M, Kitanishi K, Shimizu T. 2013. Heme-based globin-coupled oxygen sensors: linking oxygen binding to functional regulation of diguanylate cyclase, histidine kinase, and methyl-accepting chemotaxis. *J. Biol. Chem.* 288:27702–11
145. García-Moreno D, Polanco MC, Navarro-Avilés G, Murillo FJ, Padmanabhan S, Elías-Arnanz M. 2009. A vitamin B_{12}-based system for conditional expression reveals *dksA* to be an essential gene in *Myxococcus xanthus*. *J. Bacteriol.* 191:3108–19
146. Kainrath S, Stadler M, Reichhart E, Distel M, Janovjak H. 2017. Green-light-induced inactivation of receptor signaling using cobalamin-binding domains. *Angew. Chem. Int. Ed. Engl.* 56:4608–11